

Evaluating the performance of five different chemical ionization techniques for detecting gaseous oxygenated organic species

Matthieu Riva^{1,2}, Pekka Rantala¹, Jordan E. Krechmer³, Otso Peräkylä¹, Yanjun Zhang¹, Liine Heikkinen¹, Olga Garmash¹, Chao Yan¹, Markku Kulmala^{1,4}, Douglas Worsnop^{1,3}, Mikael Ehn¹

¹ Institute for Atmospheric and Earth System Research / Physics, Faculty of Science, University of Helsinki, Helsinki, 00140, Finland

² Univ Lyon, Université Claude Bernard Lyon 1, CNRS, IRCELYON, F-69626, Villeurbanne, France.

³ Aerodyne Research Inc., Billerica, MA, USA.

⁴ Aerosol and Haze Laboratory, Beijing Advanced Innovation Center for Soft Matter Science and Engineering, Beijing University of Chemical Technology (BUCT), Beijing, China

Correspondence to:

Matthieu Riva (matthieu.riva@ircelyon.univ-lyon1.fr) & Mikael Ehn (mikael.ehn@helsinki.fi)

20 **Abstract**

21 The impact of aerosols on climate and air quality remains poorly understood due to multiple factors. One of
22 the current limitations is the incomplete understanding of the contribution of oxygenated products, generated
23 from the gas-phase oxidation of volatile organic compounds (VOC), to aerosol formation. Indeed, atmospheric
24 gaseous chemical processes yield thousands of (highly) oxygenated species, spanning a wide range of chemical
25 formulas, functional groups and, consequently, volatilities. While recent mass spectrometric developments
26 have allowed extensive on-line detection of a myriad of oxygenated organic species, playing a central role in
27 atmospheric chemistry, the detailed quantification and characterization of this diverse group of compounds
28 remains extremely challenging. To address this challenge, we evaluated the capability of current state-of-the-
29 art mass spectrometers equipped with different chemical ionization sources to detect the oxidation products
30 formed from α -pinene ozonolysis under various conditions. Five different mass spectrometers were deployed
31 simultaneously for a chamber study. Two chemical ionization atmospheric pressure interface time-of-flight
32 mass spectrometers (CI-APi-TOF) with nitrate and amine reagent ion chemistries and an iodide chemical
33 ionization time-of-flight mass spectrometer (TOF-CIMS). Additionally, a proton transfer reaction time-of-
34 flight mass spectrometer (PTR-TOF 8000) and a new “Vocus” PTR-TOF were also deployed. In the current
35 study, we compared around 1000 different compounds between each of the five instruments, with the aim to
36 determine which oxygenated VOC (OVOC) the different methods were sensitive to, and identifying regions
37 where two or more instruments were able to detect species with similar molecular formulae. We utilized a
38 large variability in conditions (including different VOC, ozone, NO_x and OH scavenger concentrations) in our
39 newly constructed atmospheric simulation chamber for a comprehensive correlation analysis between all
40 instruments. This analysis, combined with estimated concentrations for identified molecules in each
41 instrument, yielded both expected and surprising results. As anticipated based on earlier studies: the PTR
42 instruments were the only ones able to measure the precursor VOC; the iodide TOF-CIMS efficiently detected
43 many semi-volatile organic compounds (SVOC) with 3 to 5 oxygen atoms; and the nitrate CI-APi-TOF was
44 mainly sensitive to highly-oxygenated organic ($\text{O} > 5$) molecules (HOM). In addition, the Vocus showed good
45 agreement with the iodide TOF-CIMS for the SVOC, including also a range of organonitrates. The amine CI-
46 APi-TOF agreed well with the nitrate CI-APi-TOF for HOM dimers. However, the loadings in our experiments
47 caused the amine reagent ion to be considerably depleted, causing non-linear responses for monomers. This

48 study explores and highlights both benefits and limitations of currently available chemical ionization mass
49 spectrometry instrumentation for characterizing the wide variety of OVOC in the atmosphere. While
50 specifically shown for the case of α -pinene ozonolysis, we expect our general findings to be valid also for a
51 wide range of other VOC-oxidant systems. As discussed in this study, no single instrument configuration can
52 be deemed better or worse than the others, as the optimal instrument for a particular study ultimately depends
53 on the specific target of the study.

54 1. Introduction

55 Atmospheric aerosols, a mixture of solid and liquid particles consisting of organic and inorganic substances
56 suspended in the air, have significant impact on climate (Albrecht, 1989; Hallquist et al., 2009;
57 Intergovernmental Panel on Climate Change, 2014; Twomey, 1977). They are also recognized to adversely
58 impact air quality and human health, representing nowadays the fifth-ranking human health risk factor,
59 globally (Gakidou et al., 2017). Depending on the regions, organic aerosol on average contributes 20-90% to
60 the submicron aerosol mass (Jimenez et al., 2009), with secondary organic aerosol (SOA) as the largest source
61 of atmospheric organic aerosol (Hallquist et al., 2009; Jimenez et al., 2009). SOA is predominantly formed
62 through the gas-phase oxidation of volatile organic compounds (VOC), producing oxygenated VOC (OVOC),
63 which can subsequently condense onto pre-existing aerosol particles. Generally, the more oxidized OVOC, the
64 lower its volatility is, and the greater is the probability of this compound to partition to the particle phase.
65 Recently, studies have provided new insights on how highly-oxygenated organic molecules (HOM) can form
66 faster than previously expected, and at high enough yields to make them a major source of condensing, or even
67 nucleating, compounds (Ehn et al., 2014; Jokinen et al., 2015; Kirkby et al., 2016; Wang et al., 2018).

68 The quantitative assessment of the impact of aerosol on climate remains poorly understood due to a
69 number of factors, including an incomplete understanding of how VOC oxidation processes contribute to new
70 particle and SOA formation (Glasius and Goldstein, 2016). Indeed, atmospheric oxidation processes can lead
71 to the formation of thousands of oxidized products from a single precursor (Glasius and Goldstein, 2016;
72 Goldstein and Galbally, 2007). As a result of these complex oxidation processes, atmospheric organic species
73 span an extremely wide range of chemical formulas, structures, and physicochemical properties. Volatilities
74 range from volatile species present only in the gas phase, via low- and semi-volatile organic compounds

75 (LVOC and SVOC), to extremely low volatility organic compounds (ELVOC) present mainly in particle phase
76 (Donahue et al., 2012). The chemical complexity of OVOC poses a major challenge in detecting, quantifying,
77 and characterizing such a large number and wide variety of organic compounds.

78 Mass spectrometric techniques, which can detect a large range of species simultaneously, are well-
79 suited to tackle these challenges. This is underlined by the major role of the mass spectrometers in improving
80 our understanding of the atmospheric chemical composition over the last twenty years (Breitenlechner et al.,
81 2017; Ehn et al., 2014; Jokinen et al., 2012; Krechmer et al., 2018; Lindinger et al., 1998; Yuan et al., 2017).
82 Proton transfer reaction (PTR) has been one of the most used medium-pressure ionization techniques since the
83 mid-1990s (Lindinger et al., 1998). Since then, the PTR-MS technique has been greatly improved in terms of
84 sensitivity, detection limit and mass resolution by introducing the PTR-TOF-MS (Yuan et al., 2017). The latest
85 version has detection limits as low as 10^7 molecules cm^{-3} . While such techniques can characterize VOC, the
86 PTR-MS technique has not been able to measure more oxygenated organic species. This is mostly due to losses
87 of these low volatile compounds in the sampling lines and on the walls of the inlet (caused e.g. by very low
88 flow rates), as the instrument was designed to primarily measure volatile compounds.

89 Several different chemical ionization mass spectrometry (CIMS) methods have been developed,
90 including medium-pressure systems like CF_3O^- -CIMS for specific detection of oxygenated VOC and SVOC
91 including hydroperoxides (Crouse et al., 2006), acetate-CIMS for selective detection of organic acids
92 (Bertram et al., 2011), and the iodide adduct ionization CIMS for the detection of wider range of OVOC,
93 including alcohols, hydroperoxides and peroxy acids (Lee et al., 2014; Riva et al., 2017). These instruments,
94 based on negative ion chemistry, can detect oxygenated gas phase compounds at concentrations as low as $\sim 10^6$
95 molecules cm^{-3} . Finally, the discovery of the HOM was possible due to the development of nitrate chemical
96 ionization source connected to an atmospheric pressure interface time-of-flight mass spectrometer (CI-APi-
97 TOF) (Ehn et al., 2014; Jokinen et al., 2012). The selectivity and high sensitivity for molecules containing
98 many functional groups (detection limit below 10^5 molecules cm^{-3}) of the nitrate CI-APi-TOF makes this
99 instrument perfect for detecting HOM and even certain radicals (e.g., peroxy radicals). As part of the rapid
100 development in gas-phase mass spectrometry, several new reagent ion chemistries have been tested over the
101 last few years. With improvements in sensitivity and/or selectivity, new methods are now able to detect a wide

102 variety of oxygenated species, including radicals and stabilized Criegee intermediates (Berndt et al., 2015,
103 2017, 2018; Breitenlechner et al., 2017; Hansel et al., 2018; Krechmer et al., 2018).

104 The selectivity and sensitivity of the different ionization chemistries makes it impossible for one mass
105 spectrometer to be able to measure the full range of VOC and OVOC present in the atmosphere. Hence, only
106 a simultaneous deployment of several mass spectrometry techniques can provide a comprehensive chemical
107 characterization of the gaseous composition. While such a multi-instrument approach maximizes the fraction
108 of organic species measured (Isaacman-VanWertz et al., 2017, 2018), a number of questions and limitations
109 can arise in both laboratory and field measurements. For instance, the extent to which instruments (i) can
110 measure species with identical molecular composition, (ii) can cover the entire range of oxygenated species,
111 (iii) can provide constant sensitivity across different conditions, have to be determined. Most studies are
112 typically limited to one, or perhaps two, mass spectrometers, and then it is also important to know which
113 fraction of the OVOC distribution these instruments are sensitive to. To our knowledge, systematic
114 comparisons of the most commonly used, or recently developed, gas-phase mass spectrometers are not yet
115 available. In this work, we compared the suitability of five different chemical ionization methods (including
116 iodide TOF-CIMS, nitrate and amine CI-APi-TOFs, a PTR-TOF and the newly developed Vocus PTR-TOF)
117 for the detection of OVOC formed from α -pinene ozonolysis during a comprehensive chamber study with
118 varying VOC, O₃, and NO_x concentrations. We characterized the time evolution of around 1000 compounds
119 and explored the capability of these instruments to measure OVOC of different oxygenation level within
120 different compound groups.

121 2. Experimental Section

122 2.1. Chamber experiments

123 Experiments were performed at the University of Helsinki in a 2 m³ atmospheric simulation Teflon (FEP)
124 chamber. The “COALA” chamber (named after the project in which it was constructed: Comprehensive
125 molecular characterization of secondary Organic Aerosol formation in the Atmosphere) was operated under
126 steady-state conditions, meaning that a constant flow of reactants and oxidants were continuously added to the
127 chamber, while chamber air was sampled by the instruments. Under the conditions used in this study, the
128 average residence time in the chamber was ~ 30 min, and the majority of conditions were kept constant for 6

129 to 12 hours before changing to new conditions. These experiments focused on the characterization of the
130 oxidation products arising from the α -pinene ($C_{10}H_{16}$) ozonolysis. α -pinene was used for the generation of
131 oxidation products because it is the most abundant monoterpene emitted by the boreal forests and is one of the
132 most important SOA precursors on a global scale (Jokinen et al., 2015; Kelly et al., 2018).

133 The experiments were conducted at room temperature ($27 \pm 2^\circ\text{C}$) and under dry conditions ($\text{RH} <$
134 1%). An overview of the measurements, as well as the experimental conditions, are presented Figure 1. α -
135 pinene was introduced to the chamber from a gas cylinder, and steady-state concentrations of α -pinene were
136 varied from 20 to 100 ppb. As alkene ozonolysis yields OH radicals (Atkinson et al., 1997), in some
137 experiments, ~ 1500 ppm of carbon monoxide (CO) was injected to serve as OH scavenger. 10 to 50 ppb of
138 O_3 was generated by injecting purified air through an ozone generator (Dasibi 1008-PC) and monitored over
139 the process of the campaign using a UV photometric analyzer (Model 49P, Thermo-Environmental). In the
140 experiments performed in the presence of NO_x , 400 nm LED lights were used to generate NO in the chamber
141 from the photolysis of the injected NO_2 . The purified air ($[\text{O}_3/\text{NO}_x]$ and $[\text{VOC}]$ reduced to less than 1 ppb and
142 5 ppb, respectively), generated by an air purification system (AADCO, 737 Series, Ohio, USA) running on
143 compressed air, was used as a bath gas. Temperature, relative humidity (RH) and pressure were monitored by
144 a Vaisala Humidity and Temperature Probe (INTERCAP® HMP60) and a differential pressure sensor
145 (Sensirion SDP1000-L025).

146 2.2. Mass spectrometers

147 We deployed five chemical ionization schemes to the COALA chamber in order to characterize the chemical
148 composition of the gas-phase oxidation products for formed from α -pinene ozonolysis. In this section, we
149 briefly present each instrument, summarized in Table 1. As each mass spectrometer has slightly different
150 working principles, references to more detailed descriptions are provided. Specific benefits and limitations,
151 which were not often discussed in earlier studies, are reviewed in section 2.4. Each of the mass spectrometers
152 were equipped with a mass analyzer manufactured by ToFwerk AG, either an HTOF (mass resolving power
153 ~ 5000) or Long-TOF (LTOF, mass resolving power ~ 10000) version.

154 In the analysis, we focused primarily on the relative behavior of the ions measured by the different
155 mass spectrometers. An absolute comparison was also performed, but this approach has larger uncertainty, as

156 the sensitivity towards every molecule is different in each of the mass spectrometers, depending on molecular
157 size, functionality, proton affinity, polarizability, etc. We attempted a rough estimate of absolute
158 concentrations for each instrument, despite the fact that with around a thousand of ions analyzed, it is evident
159 that we make no claim to be accurate for them all. As will be shown, the concentrations of gas-phase VOC and
160 OVOC vary up to 7 orders of magnitude, and therefore useful information can still be obtained even in cases
161 where concentration estimates could be off by an order of magnitude. Details about instruments used in this
162 study as well as calibrations and instrumental limitations are discussed in the following sections.

163 2.2.1. PTR-TOF

164 α -pinene concentration was measured in the COALA chamber by a proton transfer reaction time-of-flight mass
165 spectrometer (PTR-TOF 8000, Ionicon Analytik GmbH) – later referred to as “PTR-TOF”. The technical
166 details have been described in detail elsewhere (Graus et al., 2010; Jordan et al., 2009). The sample air from
167 the COALA chamber was drawn to the instrument using 2 m long PTFE tubing (6 mm o.d, 4 mm i.d.) and a
168 piece of 20 cm capillary PEEK tubing (1.6 mm o.d., 1 mm i.d.), with the sampling flow of 0.8 L/min (liters
169 per minute). The instrument was operated using a drift tube at the pressure of around 2 mbar and a drift tube
170 at the temperature of 60 degrees (°C). Drift tube voltage was kept at 600 V leading to $E/N = 145$ Td where E
171 is the electrical field strength and N the gas number density. With these settings, the primary ion isotope
172 ($H_3^{18}O^+$, 21.0221 Th) level stayed at 4500 cps (counts per second), and the mass resolving power of the HTOF
173 mass analyzer was ~ 4500 . Data were recorded using a time resolution of 10 s. The background of the
174 instrument was measured approximately every day with VOC-free air generated using a custom-made catalytic
175 converter heated to 350 °C (Schallhart et al., 2016).

176 2.2.2. Vocus

177 The Vocus PTR-TOF (proton transfer reaction time-of-flight mass spectrometer, ToFwerk AG/Aerodyne
178 Research, Inc.), later referred to as “Vocus”, is based on a new PTR-inlet design (i.e., focusing ion-molecule
179 reactor, FIMR) with sub-ppt detection limits (Krechmer et al., 2018). Sample air was drawn to the instrument
180 using 1-m long PTFE tubing (6 mm o.d, 4 mm i.d.), with a flow rate of 4.5 L/min. Most of the sample air was
181 directed to the exhaust while the actual flow to the Vocus was around 0.15 L/min. The instrument was operated
182 with 1.0 mbar drift tube pressure, the voltages being 350 V and 400 V for axial and radial voltages, respectively

183 and $E/N = 120$ Td. The Vocus was operated at a higher water flow than in Krechmer et al. (2018), resulting in
184 a decrease of the OVOC (e.g., HOM) fragmentation but also in a lower sensitivity. The signal level of the
185 instrument had some instability during the campaign, thus the primary ion signal (H_3O^+ , 19.0178 Th) varied
186 from a few hundred to few thousand cps and the isotope of the second water cluster ($H_2^{18}OH_2OH_3O^+$, 57.0432
187 Th) was around $10^4 - 10^5$ cps. The much lower signal at H_3O^+ was due to a high-pass band filter, that removes
188 most of the ions < 35 Th (Krechmer et al., 2018). The mass resolving power of the LTOF mass analyzer was
189 12000-13000 for the whole campaign. Data were recorded using a time resolution of 10 s. Zero air was
190 produced with a built-in active carbon filter and background was measured hourly except during December 15
191 – 17 due the malfunctioning of the zero air pump.

192 2.2.3. Iodide

193 Another deployed instrument was a time-of-flight chemical ionization mass spectrometer (TOF-CIMS,
194 Tofwerk AG/Aerodyne Research, Inc.), equipped with iodide (I^-) reagent ion chemistry– later referred to as
195 “Iodide”. While the molecules could be detected as deprotonated species or as adducts with I^- , we restricted
196 the analysis in this work to ions containing only an iodide adduct, which guarantees detection of the parent
197 organic compounds without substantial fragmentation. Iodide TOF-CIMS has been described previously and
198 has high sensitivity towards (multifunctional) oxygenated organic compounds (Iyer et al., 2017; Lee et al.,
199 2014). The instrument was operated at 1 L/min reagent flow rate into the Ion-Molecule Reaction (IMR)
200 chamber of the instrument. Iodide ions were generated from methyl iodide (CH_3I) using a polonium (Po-210)
201 source. Sample air was drawn to the instrument using 1 m long PTFE tubing (6 mm o.d, 4 mm i.d.) with the
202 flow rate of 2 L/min. The IMR was temperature controlled at 40°C and operated at a nominal pressure of 100
203 mbar. The instrument, equipped with an HTOF mass analyzer, was configured to measure singularly charged
204 ions from 1 to 1000 Th with a mass resolving power and time resolution of 4000 – 5000 and 10 s, respectively.

205 2.2.4. Amine/Nitrate

206 Two chemical ionization atmospheric pressure interface time-of-flight mass spectrometers (CI-APi-TOF,
207 Tofwerk AG/Aerodyne Research, Inc.) were also deployed (Ehn et al., 2014; Jokinen et al., 2012). The inlet
208 was designed to minimize wall losses through the use of coaxial sample (10 L/min) and sheath flows (~ 30
209 L/min), in order to sample (extremely) low-volatile species which are easily lost to the walls. Two types of

210 ionization schemes were utilized: the promising new amine reagent ion chemistry (Berndt et al., 2017, 2018)
211 and the more commonly used nitrate chemistry - later referred to as Amine and Nitrate, respectively. The
212 Amine has been shown to be sensitive towards a very wide range of OVOC, both closed shell species and
213 peroxy radicals, from molecules with a few oxygen atoms all the way to HOM (Berndt et al., 2018). Previous
214 work have shown that protonated amines are effective reagent ions, forming stable clusters with OVOC
215 (Berndt et al., 2018). The Nitrate, on the other hand, has mainly been used for detection of HOM (Ehn et al.,
216 2014).

217 Sample air was drawn to the instruments using a common 1 m long PTFE inlet line (19.05 mm o.d,
218 16 mm i.d.) with the flow rate being ~ 20 L/min (~ 10 L/min for each mass spectrometer). Nitrate (NO_3^-) ions
219 were formed from nitric acid (HNO_3) using an X-ray source while protonated butylamine ($\text{C}_4\text{H}_{12}\text{N}^+$) ions were
220 produced using butylamine with a 7.5 MBq Am-241 source. NO_3^- or $\text{C}_4\text{H}_{12}\text{N}^+$ ions enter the ion reaction zone
221 together with a clean sheath air flow, concentric with the sample flow, and the two do not mix turbulently. The
222 ions are then guided into the sample flow by an electrical field. The residence time in the IMR was ~ 200 ms.
223 The main reagent ions were NO_3^- (mass-to-charge 62 Th), $\text{HNO}_3\text{NO}_3^-$ (125 Th) and $(\text{HNO}_3)_2\text{NO}_3^-$ 188 Th)
224 for the Nitrate and $\text{C}_4\text{H}_{12}\text{N}^+$ (74 Th) for the Amine. Both instruments were equipped with LTOF mass analyzers
225 providing a mass resolving power of 9000 – 10000.

226 2.3. Calibration of the mass spectrometers

227 In order to estimate absolute concentrations of all detected molecules, each instrument's signals, using an
228 averaging period of 15 min, were normalized to the reagent ion signals (to eliminate the influence of changes
229 affecting all signals in the instruments, e.g., due to degrading response of the detector) followed by
230 multiplication with a scaling factor. The reagent ion quantity used for normalization is described below,
231 separately for each instrument. Normalized ion count rates are reported as normalized cps, ncps. The scaling
232 factors were derived differently for each instrument (details provided below). For Iodide, Nitrate and Amine,
233 the same factor was used for all ions in the spectrum, while for the PTR instruments the factors were different
234 depending on the type of molecules (e.g., VOC or OVOC). For the PTR instruments and the Iodide, a duty
235 cycle correction was applied to compensate for mass-dependent transmission due to the orthogonal extraction
236 of the mass analyzers. The Amine and Nitrate were calibrated by scaling a wide range of mass-to-charge based
237 on earlier studies, where duty cycle corrections had not been performed. Therefore, we did not apply such a

238 correction for the atmospheric pressure ionization mass spectrometers. Finally, we emphasize that the scaling
239 factors should not be compared between instruments as a measure of sensitivity, since multiple factors impact
240 these values, including e.g., the specific normalization approach and the chosen extraction frequency of the
241 mass analyzers.

242 The PTR-TOF was calibrated twice using a calibration unit consisting of a calibration gas mixture of
243 16 different VOC (Apel-Riemer Environmental Inc., USA) that was diluted with clean air purified by a
244 catalytic converter (1.2 L/min of zero air, and 8 sccm of standard gas), producing VOC mixing ratios of around
245 7 ppb (parts per billion) (Schallhart et al., 2016). Sensitivities were calculated to be 12.31 ncps ppb⁻¹, 27.92
246 ncps ppb⁻¹ and 30.51 ncps ppb⁻¹ based on the concentration of the monoterpenes, MVK (methyl vinyl ketone)
247 and m-/o-xylenes, respectively. PTR-TOF signals were normalized using the sum of the first primary ion
248 isotope at 21.0221 Th and the first water cluster isotope at 39.0327 Th (e.g., Schallhart et al., 2016). According
249 to common practice, the sensitivities above were scaled to correspond to a situation where the total reagent ion
250 signal equaled 10⁶ cps.

251 The Vocus was calibrated four times during the campaign using the same calibration gas mixture as
252 used for the PTR-TOF. There was variability in the sensitivity during the campaign and therefore the
253 uncertainty in the Vocus results are slightly larger than normal. Sensitivities were highest for acetone,
254 maximum around 1800 cps ppb⁻¹ and around 650 cps ppb⁻¹ for monoterpenes. α -pinene concentration was
255 retrieved using the authentic standard while the concentrations of the OVOC and C₁₀H₁₄H⁺ were estimated
256 using the calibration factor of the MVK and sum of m-/o-xylenes, respectively. MVK and m-/o-xylene
257 sensitivity was around 1700 cps ppb⁻¹ and 700 cps ppb⁻¹, respectively. Vocus signals were normalized using
258 the primary ion signal at 19.0178 Th only, as the water clusters have a negligible effect on the ion chemistry
259 inside the FIMR (Krechmer et al., 2018). Due to the high-pass filter that removes almost all the signal at
260 19.0178 Th, we do not report the normalized sensitivities (i.e., in ncps ppb⁻¹) for the Vocus, in order to avoid
261 direct comparisons with the PTR-TOF. Instead, the sensitivities above are given without normalization,
262 although a normalization was used for the final data. For the uncertainty estimates, the same applies as listed
263 above for the PTRTOF.

264 The uncertainties for the compounds that were directly calibrated are estimated to be +20 % for PTR-
265 TOF and Vocus. For other compounds, the uncertainties are much higher due to uncertain ionization

266 efficiencies and potential fragmentation of the compounds with unknown structures. For example, we used
267 sensitivity of MVK for all oxygenated monoterpenes even though all those compounds may have very different
268 fragmentation patterns, transmission rates and/or proton transfer reaction rates from each other. Therefore, we
269 refrain from quantitative estimates of the uncertainties for these species.

270 The Iodide was calibrated twice during the campaign (December 15 and 23) by injecting known
271 amounts of formic acid to the instrument. Due to unknown reasons, the response of the Iodide decayed
272 throughout the campaign, and therefore only data measured before December 17, when a stronger drop
273 occurred, was included for the direct comparison of the non-nitrate OVOC. While normalization should
274 compensate for this type of behavior, this particular instrument utilized a time-to-digital converter (TDC)
275 acquisition card, which meant the primary ion peak was heavily saturated. Lacking any isotopic signatures for
276 I^- , we found that utilizing a region of the rising edge of the I^- signal (126.5-126.65 Th) provided a reasonable
277 correction to our data. The sensitivity without normalization was 1.0 cps ppt⁻¹ for formic acid, and following
278 the normalization, this sensitivity was applied for all ions throughout the period where Iodide data was included
279 in the analysis. We acknowledge that this brings with it a large uncertainty, as the Iodide has sensitivities
280 ranging over a few orders of magnitude depending on the specific molecule (Lee et al., 2014), and refrain from
281 quantitative uncertainty estimates, as in the case for the PTR instruments above.

282 Standards for OVOC compounds measurable by the Nitrate are still lacking, and this instrument was
283 therefore not directly calibrated during the campaign. However, to be able to roughly estimate concentrations,
284 a calibration was inferred by assuming that the molar yield of HOM, i.e., molecules with six or more oxygen
285 atoms, during α -pinene ozonolysis experiments was 5%. Different values have been reported for the HOM
286 yield in this system, ranging from slightly above to slightly below 5% (Ehn et al., 2014; Jokinen et al., 2014,
287 2015). Clearly such an approach yields large uncertainties, and we estimated it here to roughly $\pm 70\%$. Earlier
288 work with more direct calibrations reported an uncertainty of $\pm 50\%$ (Ehn et al., 2014), and the added 20 p.p.
289 in this work reflects the increased uncertainty in scaling the sensitivity based on expected HOM yields. This
290 method requires knowledge on the wall loss rate of HOM in the COALA chamber, which was estimated to be
291 $1/300\text{ s}^{-1}$ in our study. This estimate is based on a rough scaling to a slightly smaller chamber (1.5 m^3) with
292 active mixing by a fan, where the loss rate was measured to be 0.01 s^{-1} (Ehn et al., 2014). As our chamber is
293 larger, and our mixing fan was only spinning at a moderate speed, we estimated the loss rates to roughly 3

294 times lower. The resulting calibration coefficient was $2 \cdot 10^{10}$ molecules cm^{-3} ncps^{-1} , which is similar as in
295 previous studies (Ehn et al., 2014; Jokinen et al., 2012). As for Nitrate, the Amine was also not calibrated
296 directly, and in order to achieve an estimate of the concentrations measured by this instrument, we scaled the
297 sensitivity of the Amine to match that of the Nitrate for specific HOM dimers ($\text{C}_{19}\text{H}_{28/30}\text{O}_{12-17}$ and $\text{C}_{20}\text{H}_{30/32}\text{O}_{12-}$
298 $_{17}$), which were found to correlate very well between the two instruments (as described in more detail in the
299 Results section). This approach gave a calibration factor of $6 \cdot 10^8$ molecules cm^{-3} ncps^{-1} , with similar
300 uncertainty estimates as for the Nitrate. In the CI-APi-TOFs, the calibration factor is generally close to 10^{10}
301 molecules cm^{-3} ncps^{-1} , but as discussed later in section 3.1, the Amine reagent ion was considerably depleted
302 during the experiments, which led to the relatively low calibration factor. As mentioned earlier, the scaling
303 factors should not be compared directly between instruments. The lower value for the Amine is a result of the
304 normalization rather than an indication of higher sensitivity. This reagent ion depletion also means that the
305 most abundant species were most likely no longer responding linearly to concentration changes, and therefore
306 their concentrations can be off by an order of magnitude or more.

307 2.4. Instrumental limitations and considerations

308 In this section we aim at highlighting some of the limitations involved when characterizing and quantifying
309 OVOC measured by online mass spectrometers. The list below is not exhaustive, but addresses several issues
310 that are relevant for the interpretation of our results.

311 2.4.1. Mass resolving power

312 One major limitation for all of the mass spectrometers described above, is the mass resolving power, ranging
313 from 4000 to 14000. Even though the new generation of LTOF mass analyzers with higher resolving power
314 can enhance the separation of measured ions, it remains challenging to accurately identify and deconvolve the
315 elemental composition of many ions. Indeed, it is common for one CIMS mass spectrum to include more than
316 1000 different ions. For high-resolution (HR) peak identification and separation, firstly one needs to generate
317 a list of ions, i.e., “peak list”. Its construction can be time-consuming even if only based on one single spectrum,
318 and once conditions change, different ions may appear. For measurements lasting weeks or months, it is nearly
319 impossible to assure that all ions are correctly identified and fitted. If the peak list contains too few ions
320 compared to reality, signals from non-fitted ions will assign the adjacent ions with artificially high signals. On

321 the contrary, if too many closely lying ions are included in the peak list, even small errors in the mass axis
322 determination can cause signal to be fitted to specific ions even though their signals are non-existent. In such
323 extreme cases, with closely overlapping ions, traditional HR analysis becomes impossible.

324 While less selective detection techniques can sound more useful to monitor and characterize OVOC,
325 spectra acquired using such ionization techniques (e.g., PTR, Iodide or Amine), pose a significant challenge
326 for data analysis and may ultimately provide even less useful information. Statistical analysis techniques can
327 be used in order to better constrain the uncertainties associated with peak fitting, as recently proposed (Cubison
328 and Jimenez, 2015; Stark et al., 2015). These previous studies pointed out that the uncertainties related to the
329 peak fitting can become significant if the overlapping peaks are separated by less than a full-width at half-
330 maximum (Cubison and Jimenez, 2015). This is very often the case for CIMS instruments, and the more the
331 ions overlap, the larger the uncertainty is. Peak fitting becomes increasingly problematic as molecular masses
332 increase, since the number of potential ions increases dramatically with mass.

333 2.4.2. Ionization, declustering and fragmentation

334 The response of a mass spectrometer to a certain compound is to first approximation a result of two factors:
335 the ionization probability of the neutral molecule, and the detection probability of the formed ion. The
336 ionization process is largely controlled by the stability of the products compared to the primary ions, whether
337 a question of adduct formation or (de)protonation processes. Different reagent ion chemistries have been
338 studied computationally in recent years, successfully reproducing several observations (Berndt et al., 2017;
339 Hyttinen et al., 2015, 2018; Iyer et al., 2016). While a neutral molecule can bind to a reagent ion at the collision
340 limit, the adduct can undergo collision-induced dissociation (i.e., declustering) during transport through the
341 interface to the high vacuum in the mass analyzer. Ultimately, the binding strength of the adduct and the energy
342 of the collisions in the mass spectrometer will define the survival probability of the ions. To address this issue,
343 procedures have been proposed, e.g., to probe the response of adducts to different collision energies (Isaacman-
344 VanWertz et al., 2018; Lopez-Hilfiker et al., 2016), providing critical information on the sensitivity of the
345 instrument.

346 Similarly to declustering, (de)protonated compounds can undergo fragmentation reactions where
347 molecular bonds are broken. For example, the detection of monoterpenes ($C_{10}H_{16}$) using PTR instruments often
348 shows equally large signals at the parent ion ($C_{10}H_{17}^+$) and at a fragment ion ($C_6H_9^+$). Also, Iodide adducts

349 have been shown to cause molecules to fragment, as in the case of peroxy acids decomposing to carboxylate
350 anions (Lee et al. 2014). Both declustering and fragmentation processes are associated with the optimization
351 of the voltages of each instrument, which is performed by the instrument operator (Breitenlechner et al., 2017;
352 Krechmer et al., 2018; Lopez-Hilfiker et al., 2016). While using voltage scans to probe such processes is
353 possible, and even desirable, performing, interpreting and utilizing the results, across the mass spectrum and
354 across different conditions, remains challenging and has only been utilized in a few studies to date (Isaacman-
355 VanWertz et al., 2018; Lopez-Hilfiker et al., 2016).

356 2.4.3. Quantification

357 For quantification, the instrument sensitivity is generally determined via calibration standards, while a
358 background level was measured by zero air. The challenges involved in these procedures are highly dependent
359 on the type of compounds to be quantified. As an example, we discuss three kinds of molecules with different
360 volatility: VOC, SVOC and ELVOC.

361 (a) VOC: volatile species are relatively easy to quantify since they can be contained in gas bottles or easily
362 evaporated from standard samples in known quantities. Their responses are also fast due to negligible
363 adsorption/evaporation from walls.

364 (b) SVOC: Many semi-volatile organic compounds (SVOC) are commercially available and can be
365 evaporated in known amounts from liquid standards into the gas phase. However, the nature of SVOC
366 results in both condensed and gas phases for these species, meaning that once clean air is introduced, the
367 signal of SVOC will often show a gradual decay over minutes, or even hours, due to evaporation of the
368 ‘leftover’ from surfaces in the inlet lines and the inlet itself (Pagonis et al., 2017). The procedure to
369 determine the “correct” blank is not trivial, and the blank will look different depending on whether it is
370 done at the entrance of the instrument or at the sampling inlet, and depending on the duration of the blank
371 measurement itself. Another related challenge for SVOC quantification is that temperature fluctuations of
372 a few degrees may cause net evaporation (temperature increasing) or condensation (temperature
373 decreasing) of SVOC from sampling lines and the inlet.

374 (c) ELVOC: For ELVOC, finding standard compounds for calibration remains extremely difficult. Most
375 organic compounds, including hydroperoxide or acid, with such low volatility are likely to decompose
376 before evaporating. Thus, their quantification is often inferred from other similar compounds. For the

377 nitrate CI-API-TOF, sulfuric acid is often used for calibration, by forming it in-situ from SO₂ (Kürten et
378 al., 2012). This is, to some extent, a similar approach as we took for the Nitrate in this work, scaling it to
379 the estimated HOM yield, as both methods require knowledge of formation rates from the initial precursors
380 and loss rates of the formed compound of interest. Other studies have used permeation sources of
381 perfluorinated carboxylic acids, which are semi-volatile, yet found to bind strongly to nitrate ions (Ehn et
382 al., 2014; Heinritzi et al., 2016). However, while the calibration is complicated, the blank measurements
383 are often not even needed, for exactly the same reasons. Whatever contaminants might be present in the
384 system, most are irreversibly lost to instrument surfaces and unable to evaporate into the gas phase due to
385 the extremely low vapor pressures. Potential oxidation processes occurring inside the mass spectrometer
386 may be an exception, but to our knowledge, this has not been reported as a large concern for ELVOC.

387 In addition to the list above, the response of an instrument to specific molecules may vary according to the
388 conditions at which they were sampled. Temperature (change) was listed as one consideration, and water
389 vapor, or relative humidity (RH), is another important limitation for several mass spectrometers described
390 above (Breitenlechner et al., 2017; Krechmer et al., 2018; Kürten et al., 2012; Lee et al., 2014; Li et al., 2018).
391 For chemical ionization techniques, the water vapor can either compete with the OVOC ionization, leading to
392 decrease of the sensitivity, or stabilize the adduct resulting in an increase of the sensitivity. Alternatively, if a
393 compound forms a very stable complex, it may have an adduct formation efficiency that is independent of
394 water vapor. If the sensitivity is RH-dependent, calibrations and blanks should optimally be performed at the
395 same RH as the sampling in order to be representative. This, in turn, may cause considerable practical
396 challenges for both RH control and calibration and blank cleanliness.

397 In summary, recent computational and experimental work has shown that many approaches exist for
398 optimizing the ability of CIMS instruments to quantify OVOC, including different blanks, calibration methods,
399 voltage scans, etc. However, all these approaches are very rarely utilized in a single study, simply due to the
400 immense time and effort required, both during the experiments and during the data analysis, where the results
401 of all steps need to be incorporated. Ultimately, each study needs to prioritize between producing larger
402 amounts of data (i.e., performing more measurements) with less capability for detailed quantification, or to
403 produce a smaller amount of data with more accurate quantification.

404 3. Results and discussion

405 We applied our five CIMS instruments at the COALA chamber over a period of nearly one month, where we
406 tried to provide different types of atmospherically relevant oxidation conditions for α -pinene. With such a high
407 variability in conditions, we compared signals between the mass spectrometers more robustly, even though
408 certain limitations were inevitable. For example, it is often the case that mass spectra will show some signal at
409 almost every mass, which can be due to multiple reasons, and it is important to separate when the signal is
410 truly from the sampled air and not from some internal background or contamination. Similarly, one needs to
411 assess whether the instrument is measuring the majority of the species with the same elemental composition,
412 or only detecting a small subset of those compounds due to specific selectivity for one isomer. In addition, an
413 instrument may be able to detect a certain molecule, but the resulting signal remains unreliable. This may be
414 the case if the sensitivity is extremely low for the molecule, or if the peak is close to a much larger unrelated
415 signal, which will create large interferences when performing HR fitting. In both cases the signal is likely to
416 be influenced by different types of noise.

417 First, we performed correlation analyses in order to identify signals which were physically
418 meaningful. We conducted the analysis with the whole dataset (a total of ~ 1000 ions in each instrument) rather
419 than selectively focusing on individual ions. This comprehensive approach utilized more data, but also resulted
420 in larger uncertainties as not all fitted ions could be validated for all CIMS. From the correlation analysis we
421 identified when two instruments agree, i.e., observing identical elemental compositions and having a similar
422 temporal behavior, concerning some group of compounds. From a subsequent absolute comparison, we
423 estimated which chemical ionization method was likely to be detecting a certain group of compounds more
424 efficiently.

425 3.1. Instrument comparisons: correlations

426 3.1.1. Medium pressure ionization mass spectrometers

427 Peak fitting was performed utilizing the Igor-based Tofware or Matlab-based Toftools software (Junninen et
428 al., 2010) for ion mass-to-charge up to ~ 600 Th, depending on the mass spectrometers. To select which ions
429 to fit (i.e., include in the peak lists), both the exact masses and the isotopic distributions were used as criteria.
430 A Pearson correlation coefficient R , was calculated between molecules having the same elemental composition

431 measured by the different instruments. As a practical example, the time series of $C_{10}H_{16}O_3$ measured by Vocus
432 and Iodide are shown in Figure 1C, and the time series correlation for this compound between the two
433 instruments was $R = 0.85$. For later comparisons we will use R squared, and in this case $R^2 = 0.73$. For Iodide,
434 the data set covered only the first half of the campaign, but the other instruments covered nearly the whole
435 period. This includes a wide variety of conditions, with and without NO_x , and therefore high correlations are
436 very suggestive of two instruments measuring the exact same compound(s) at that specific elemental
437 composition. However, as an increase in α -pinene is likely to increase almost all measured OVOC signals to
438 some extent, low positive correlations can arise artificially and should not be over-interpreted. Due to the
439 selectivity and the sensitivity of the ionization methods, not all ions were observed in all the different
440 instruments, and thus only a certain fraction of the identified compounds can be compared between mass
441 spectrometers.

442 Figure 2 shows the correlation analysis for the medium-pressure chemical ionization mass
443 spectrometers, with marker size scaled by R^2 . In those figures, the abscissa represents the measured mass-to-
444 charge ratio of the compounds and the y-axis their mass defect, which is calculated as the exact mass of the
445 compound minus the mass rounded to the closest integer (Schobesberger et al., 2013). For example, the mass
446 of $C_{10}H_{16}O_3$ is 184.110 Da and the mass defect is + 0.110 Da. The contribution of the reagent ions has been
447 removed in the different Figures. A mass defect diagram helps to separate the molecules into two dimensions
448 and allows some degree of identification of the plotted markers.

449 As expected, the PTR-TOF and the Vocus are strongly correlated for compounds with low (0-3)
450 oxygen number (Figure 2A). Contrariwise, only a few compounds were identified by the PTR-TOF and the
451 Iodide with a fairly good correlation (i.e., $R^2 > 0.5$). The correlating compounds included small acids such as
452 formic and acetic acid. As discussed earlier, the inlet of the PTR-TOF is not well designed to sample OVOC
453 having low volatility, which explained the lack of correlations for larger and more oxidized products between
454 the PTR-TOF and the Nitrate CI-APi-TOF. The molecules with the lowest correlations ($R^2 < 0.2$) were not
455 included in the plots, as the intention is to show regions where instruments agree. If an ion is included in a
456 peak list, it will always be fit, and thereby a value of $R^2 > 0$ is always expected, filling markers throughout the
457 MD-mass space.

458 In addition to VOC, the Vocus was able to measure a large range of OVOC (150-300 Th) as revealed
459 in Figure 2B, displaying a very good correlation with species identified by the Iodide. Indeed, most of the
460 identified compounds have $R^2 > 0.7$. As noted earlier, several different experimental conditions were tested
461 (Figure 1), and these high correlations indicate that both instruments were likely sensitive to the same
462 compounds. In other words, as good correlation was seen in this mass range for nearly all compositions, the
463 Iodide and the Vocus did not seem to be strongly impacted by the exact chemical conformation of the organic
464 compounds. Interestingly no dimers (mass-to-charge > 300 Th) were observed with the Vocus, which suggests
465 some potential limitation of the instrument or the used settings. As a result, very limited correlation was
466 observed between compounds measured by the Vocus and the Amine or Nitrate CI-API-TOFs. The two main
467 exceptions being $C_5H_6O_7$ (178.011 Da) and $C_7H_9NO_8$ (235.033 Da). Note that the latter is less clear, as the
468 correlation is nearly identical between three instruments (Nitrate, Vocus and Iodide). The lack of correlation
469 was not only due to lack of ion transmission at higher masses in the Vocus, since the instrument was able to
470 detect some ions up to 400 Th, including $C_{10}H_{30}O_5Si_5H^+$ and $C_{19}H_{29}O_6NH^+$. One possibility was that since the
471 compounds above ~ 300 Th were likely to contain hydroperoxides, or in the case of dimers, organic peroxides,
472 the ions might may have fragmented before detection in the Vocus, either during the protonation or due to the
473 strong electric fields in the Vocus FIMR. In the case of HOM monomers with more than 7 oxygen atoms, an
474 additional limitation comes from more abundant and closely overlapping ions in the spectra, impacting the
475 accurate fitting of these ion signals in the Vocus. From our data set, it was not possible to determine the exact
476 cause(s) for this lack of sensitivity for larger molecules in the Vocus, but it is possible that changes in
477 instrument operating conditions can extend the range of molecules detectable using the Vocus in future studies.

478 As shown in Figure 2C, the Iodide was capable of measuring ions with larger masses (i.e., above 300
479 Th) indicating the detection of more complex (e.g., dimers) and oxygenated compounds than the Vocus. This
480 was the case in spite of the lower flow rate for the Iodide than the Vocus, and thus less optimal for sampling
481 of low-volatile species (Table 1). The Iodide seemed to have the widest detection range of the mass
482 spectrometers deployed in this study, showing high correlation with other instruments for organic molecules
483 from C_1 (like formic acid) to C_{20} , as long as the molecules had at least two oxygen atoms. This is in line with
484 earlier findings that the Iodide is sensitive to most species that are polar or have polarizable functional groups
485 (Iyer et al., 2017; Lee et al., 2014). However, the correlation with the CI-API-TOFs was still somewhat limited

486 ($R^2 < 0.7$) for HOM monomers and dimers. One reason may have been that these HOM contain peroxy acid
487 functionalities, which have been shown to undergo reactions in the Iodide TOF-CIMS (Lee et al., 2014). In
488 this work, we only analyzed the ions containing Γ as these were believed to be the ones where the parent
489 molecule remained intact. Another reason for lower correlation was the fact that Γ is less selective than other
490 ionization methods resulting in many overlapping peaks at the same integer mass and ambiguous peak fitting
491 (Lee et al., 2014; Stark et al., 2015, 2017), similar to the case in the Vocus. This means that although the Iodide
492 and/or the Vocus might be able to charge a specific molecule, and it would not fragment before detection, the
493 ion may remain unquantifiable due to highly ambiguous peak fitting as a result of multiple overlapping signals.

494 3.1.2. Atmospheric pressure interface mass spectrometers

495 Figure 3 shows similar comparisons as in Figure 2, now for the Nitrate (Figure 3A) and the Amine (Figure
496 3B). Interestingly, these two instruments show excellent correlation ($R^2 > 0.9$) for dimeric products (molecules
497 within 350-500 Th), but showed mostly low correlations ($R^2 < 0.6$) with other instruments in the monomer
498 range. The Nitrate had some agreement with the Iodide for certain monomer compounds, but in the HOM
499 monomer range where the Nitrate generally saw its largest signals (C_{10} molecules with 7 to 11 oxygen atoms;
500 Ehn et al., 2014), none of the other instruments showed strongly correlating signatures.

501 Despite showing signals at almost all OVOC, the Amine presented low correlations for all OVOC
502 except the dimers. In the Amine the reagent ion was greatly depleted due to the relatively high signals (Figure
503 4), likely leading to a non-linear response for most of the OVOC, apparently with the exception of the HOM
504 dimers. It may be that the amine reagent ion formed extremely stable clusters with these dimers, and thus any
505 collision involving these dimers with the reagent ion (regardless of whether already clustered with an OVOC)
506 in the IMR lead to an amine-dimer cluster. While the Amine showed very low correlation with the other
507 instruments for most molecules, it has been demonstrated to be an extremely useful detector of both radicals
508 and closed shell OVOC under very clean, low-loading flow tube experiments (Berndt et al., 2017, 2018). In
509 other words, it can provide information on a wide variety of OVOC, but to obtain quantitative information, the
510 amine CI-APi-TOF has to be used in very diluted system (with very clean air) and at low loadings. Determining
511 more explicitly the limitations requires further studies, but as a rough approximation, the typical CI-APi-TOF
512 sensitivity of $\sim 10^{10}$ molecules cm^{-3} ncps^{-1} means that when sampling detectable molecules at 10^{10} molecules
513 cm^{-3} (~ 0.4 ppb), these molecules will have ion signals of equal abundance as the reagent ions. Consequently,

514 once the concentration of measurable molecules exceeds roughly 100 ppt, the CI-APi-TOF may no longer be
515 an optimal choice. For the Nitrate CI-APi-TOF, which mainly detects HOM with short lifetimes due to their
516 low volatilities, this has rarely been a limitation, but for less selective reagent ions, like amines, this can be an
517 important consideration.

518 3.2. Instrument comparisons: concentration estimates

519 Concentrations of the identified compounds were estimated for all the different instruments, as described in
520 section 2.6. It should be noted that no separate inlet loss corrections were applied. The estimations for the
521 results of PTR-TOF and the Vocus are the most reliable as both instruments were calibrated using authentic
522 standards with a proven method, while larger uncertainties in the total measured concentrations are expected
523 for the Iodide and the CI-APi-TOFs.

524 With around 1000 identified ions for each instrument, except for the PTR-TOF, we decided to focus
525 our attention in this section on a few particular compound groups: the most abundant C₁₀-monomers (i.e.,
526 C₁₀H_{14/16}O_n), C₁₀-organonitrates (C₁₀H₁₅NO_n) and dimers (C₂₀H₃₂O_n). For the non-nitrate compounds, the
527 concentrations were measured during a steady-state conditions of December 9 from 15:30 to 23:00 with [O₃]
528 = 25 ppb and [α -pinene] = 100 ppb) during period I (Figure 1 in blue). The organonitrate concentrations were
529 compared using steady-state conditions of December 20 from 02:45 to 07:45 with [O₃] = 35 ppb, [α -pinene] =
530 100 ppb and NO = 0.5 ppb, during period IV (Figure 1 in purple). Figures 5A-D show the concentrations of
531 the selected species as a function of oxygen number in the molecules. While we again emphasize that all the
532 concentrations were only rough estimates, these plots painted a similar picture to the correlation analysis, as
533 described in more detail in the next paragraphs.

534 Focusing first on the non-nitrate monomers (Figures 5A-B), for compounds with zero or one oxygen
535 atoms, the PTR-TOF agreed well with the concentration estimated by the Vocus, while molecules with more
536 than two oxygen atoms were already close to, or below, the noise level of the PTR-TOF. In contrast, as the
537 number of oxygen atoms in the molecule reached two or more, the Iodide signal increased, and for most
538 compounds showed concentrations similar to the Vocus. These two instruments agreed on concentration
539 estimates fairly well all the way up to an oxygen content of around 9 oxygen atoms, where the measured signals
540 were close to the instruments' noise levels. However, when comparing to the Nitrate, which is assumed to have
541 good sensitivity for HOM with 7 or more oxygen atoms, the concentrations suggested by the Vocus and Iodide

542 for the O₇ and O₈ monomers were very high. We preliminarily attributed this to an over-estimation of the
543 concentrations of HOM by these two instruments, possibly due to higher sensitivities towards these molecules
544 as compared to the compounds used for calibration (i.e., MVK). We also did not correct for potential
545 backgrounds using the blanks for the Iodide, although measured, since the variability in the blank
546 concentrations (see also discussion in section 2.4) was large enough to cause artificially high fluctuations in
547 the final signals. Therefore, we opted to not include such a correction, but also note that even if half the signal
548 at a given ion was attributable to background in the Iodide, then it would only have a small impact on the
549 logarithmic scales used in Figure 5. Other possible reasons for this discrepancy was that the Iodide and Vocus
550 were able to detect isomers that the Nitrate was not, or that the Nitrate sensitivity was under-estimated.
551 However, considering that the Nitrate HOM signal was scaled to match a 5% molar HOM yield, it was unlikely
552 that the HOM concentrations can be considerably higher than this. Other estimated parameters involved in the
553 formation and loss rates of HOM also had uncertainties, but we did not expect any of them to be off by more
554 than 50%. This concentration discrepancy thus remained unresolved, and will require more dedicated future
555 studies.

556 Finally, the quantities estimated using the Amine are significantly lower (1-2 orders of magnitude) for
557 all monomers when comparing to the other instruments. This was presumably related to the titration of the
558 reagent ion, which meant that the majority of charged OVOC will undergo multiple subsequent collisions with
559 other OVOC, potentially losing their charge in the process. The Nitrate had, as expected, very low sensitivity
560 towards less oxygenated compounds, and its highest detection efficiency for HOM (i.e., molecules with at least
561 6 oxygen atoms).

562 The organonitrate comparison in Figure 5C suggested that both the Vocus and the Iodide were efficient
563 at detecting these compounds, as both instruments agreed well ($R^2 > 0.7$) for C₁₀-organonitrates with 5 to 10
564 oxygen atoms. While organonitrates have been detected before using the Iodide (Lee et al., 2016), this was the
565 first observation that also the Vocus can detect such compounds efficiently. However, we cannot exclude that
566 such compounds undergo fragmentation within the drift tube as commonly observed in other PTR instruments
567 (Yuan et al., 2017). For larger oxygen content, the Nitrate again seemed to be most sensitive, showing clear
568 signals above 10 oxygen atoms, where the previous instruments were already close to noise levels. The Amine
569 seemed worse at detecting organonitrates compared to non-nitrate monomers.

570 Neither of the PTR instruments were able to detect any dimers in this study within their measurement
571 ranges (up to 320 Th for PTRTOF). The Amine and the Nitrate were able to quantify the widest range of HOM
572 dimers, while the Iodide was able to detect less oxidized dimers (Figure 5D). Based on the concentration
573 estimates, the Amine's detection range also extended to less oxidized dimers than the Nitrate, as has already
574 been shown by Berndt et al. (2018). Dimers measured by the Iodide were more abundant than the ones detected
575 by the Amine, but already from the monomer comparisons we speculated that the Amine might be
576 underestimating concentrations while the Iodide might be overestimating them. With the data available to us,
577 we can only speculate on the relative sensitivities of the instruments able to detect dimers, especially with the
578 Vocus providing no support to the comparison.

579 One aspect lending credibility to the Amine dimer data, in addition to the good time series correlation
580 with the Nitrate, was the odd-even oxygen atom patterns visible both in the Amine and Nitrate data. Such a
581 pattern is to be expected, since the 32 hydrogen atoms in the selected dimers indicates that they have been
582 formed from RO₂ radicals where one had 15 hydrogen atoms (which is what ozonolysis will yield, following
583 OH loss) (Docherty et al., 2005; Lee et al., 2006; Ziemann and Atkinson, 2012), while the second RO₂ had 17
584 hydrogen atoms (which is the number expected from OH oxidation of an alkene where OH adds to the double
585 bond). The first RO₂ from ozonolysis had 4 oxygen atoms, and further autoxidation will keep an even number
586 of oxygen atoms, while the opposite was true for the OH-derived RO₂ which started from 3 oxygen atoms. In
587 other words, the major dimers from this pathway should contain an odd number of oxygen atoms after
588 combination. In the case of C₂₀H₃₀O_n dimers, mainly formed from two ozonolysis RO₂, the pattern was
589 expected to show peaks at even n, which is also the case (not shown).

590 Such odd-even patterns for the oxygen content was not visible in the Iodide, but the reason remained
591 unknown. It was possible that the dimers detected by the Iodide might be formed via other pathways, where
592 such a selectivity did not occur. This topic should be explored further in future studies, since dimers formed
593 from the oxidation of biogenic compounds are important for new-particle formation, and it is therefore critical
594 to accurately identify and quantify the formation and evolution of different types of dimers. To date, both
595 dimers measured by Iodide (Mohr et al., 2017) and Nitrate (Tröstl et al., 2016) have been found to be important
596 for particle formation from monoterpenes.

597 3.3. Performance in detecting oxygenated species

598 Figure 6 summarizes our results and depicts the performance of each mass spectrometer in detecting monomer
599 and dimer monoterpene oxidation products. Molecules of $C_{10}H_{16}O_n$, $C_{10}H_{15}NO_n$ and $C_{20}H_{30}O_n$ were provided
600 as examples. We emphasized that the oxygen content alone was not the determining factor for whether a certain
601 type of mass spectrometer will detect a compound, but we utilized this simplified representation in order to
602 provide an overview of the performances of the different chemical ionization schemes. The results were
603 primarily based on the correlation analysis from section 3.1, and as apparent from the y-axis, this comparison
604 was only qualitative. However, our aim was to provide an easy-to-interpret starting point, especially for new
605 CIMS users wanting to compare different available techniques.

606 For monomer compounds without N-atoms, shown in Figure 6A, the PTR-TOF was limited to the
607 detection of VOC, while the Vocus was additionally able to measure a large range of OVOC, up to at least 5-
608 6 oxygen atoms. The Iodide detected OVOC with oxygen content starting from ~ 3 atoms, but did not seem to
609 efficiently observe HOM monomers (i.e., $C_{10}H_xO_{>7}$). While being a very promising instrument for a broad
610 detection of OVOC, the performance of the Amine was limited in our study due to a significant drop of the
611 reagent ion to $\sim 40\%$ of the total signal. Therefore, the Amine was marked with a shaded region rather than a
612 line, with the lower limit based roughly on its usefulness under the conditions we probed, while the upper limit
613 was an estimate based on findings in a cleaner system with low loadings (Berndt et al., 2018). Finally, the
614 Nitrate was mainly selective towards HOM. The detection and quantification of monomeric OVOC containing
615 5 to 8 oxygen atoms remained as the most uncertain, since there were inconsistencies in both concentration
616 and correlation between the Nitrate, measuring the more oxygenated species, and the Vocus/Iodide, which
617 detected the less oxidized compounds.

618 In Figure 6B, the suitability for the different instruments was plotted for organonitrate monomers. The
619 Vocus efficiently detected the less oxidized organonitrates, while the Iodide displayed a good sensitivity for
620 the same compounds, with the exception of the least oxygenated ones. For larger number of oxygens, the
621 Nitrate again seemed the most suitable method. For dimers (Figure 6C), neither of the PTR techniques showed
622 any ability to detect these compounds in our study. We did not extend the lines all the way down to $n = 0$ for
623 the compounds, as it was still possible that these methods can be able to detect the least oxidized and most
624 volatile C_{20} compounds, which might not have been present during our experiments. The Iodide showed some

625 correlation with the Nitrate, but had good signals mainly in the range of dimers with 4 to 8 oxygen atoms. The
626 Amine and Nitrate correlated well for the most oxidized dimers, suggesting good suitability for dimer detection
627 of HOM dimers. The Amine concentrations stayed high, with the expected odd-even pattern in oxygen number,
628 even at lower oxygen content than the Nitrate, and therefore the suitability extended further towards lower O-
629 atom contents. Again, the shaded area was based on a combination of our findings and those of Berndt et al.
630 (2018).

631 The results in Figure 6 are based on the α -pinene ozonolysis system. While we will not speculate too
632 much about the extent to which these findings can be extrapolated to other systems, certain features will remain
633 similar also for other atmospherically relevant reactions. For example, the most oxidized gaseous HOM species
634 will likely have been formed through autoxidation processes, which means that they will contain
635 hydroperoxide functionalities, and could thus be detectable by the Nitrate. Likewise, the HOM, and in
636 particular the dimers, will very likely have low volatilities, requiring high sample flows with minimal wall
637 contact, as in the case of the Eisele-type CI inlets used in the Nitrate and Amine. Several other key features are
638 also expected to be valid in different VOC-oxidant systems, and therefore we believe that our findings are
639 relevant also for many other reaction partners.

640 As a final test for each instrument, we estimated how much of the reacted carbon (in ppbC) the
641 different mass spectrometers can explain. As shown in Figure 7, both the Iodide and Vocus seemed to capture
642 most of the reacted carbon, within uncertainties. The concentration determined using the Vocus was
643 overestimated, explaining more carbon than was reacted. Out of the largest contributors to the reacted carbon,
644 pinonaldehyde ($C_{10}H_{16}O_2$) was not efficiently detected by Iodide, but otherwise most of the abundant
645 molecules were quantified by both Vocus and Iodide. Any carbon lost by condensation to walls or particles
646 would not have been quantifiable by any of the instruments in this study. While the Nitrate was calibrated with
647 an assumption that it can measure 5% of the reacted α -pinene, it only detected less than a tenth of that amount.
648 The reason was that the HOM it can detect were quickly lost to walls (or particles), and thus the gas-phase
649 concentration was not equivalent to the branching ratio of the VOC oxidation reaction. In fact, and as revealed
650 by the slow changes in the times series in Figure 7D, most of the carbon ultimately measured by the Nitrate
651 was semi-volatile, as such compounds accumulated and reached higher concentration in the chamber, unlike
652 HOM. Thus, while the Nitrate was able to detect a critical group of OVOC from an aerosol formation

653 perspective, i.e., HOM, for carbon closure studies (Isaacman-VanWertz et al., 2017, 2018) it will be of limited
654 use. This again highlights the need to first determine the target of a study before deciding which CIMS
655 technique is the most useful. For the closure comparison in our study, the overestimations emphasized the need
656 to perform calibration with an extensive set of OVOC, ideally with monoterpene-oxidation products, in order
657 to better constrain the sensitivity of the products of interest. The study by (Isaacman-VanWertz et al., 2018),
658 as the only study to achieve full carbon closure during chamber oxidation of α -pinene by OH, also successfully
659 utilized voltage scanning to determine sensitivities of each compound.

660 4. Conclusions

661 The primary goal of this work was to evaluate the performance of 5 chemical ionization mass spectrometers
662 (PTR-TOF, Vocus PTR, Iodide TOF-CIMS, Amine CI-APi-TOF and Nitrate CI-APi-TOF) in the
663 identification and quantification of a wide variety of products formed in the ozonolysis of α -pinene. In addition,
664 we wanted to estimate the capabilities of the newly developed Vocus PTR in measuring OVOC species. By
665 comparing the regions of coverage of the instruments across multiple experimental conditions (i.e., in different
666 O₃, VOC, NO and OH radical concentrations) we demonstrated that current instrumentation captures nearly
667 the entire range of OVOC, spanning from VOC to ELVOC. The PTR-TOF was only able to measure the most
668 volatile compounds, while the Vocus appeared to be able to measure both VOC and most of the OVOC up to
669 5 to 6 oxygen atoms. In combination with the Iodide and Nitrate, most of the OVOC range can be measured.
670 The Iodide showed good overlap with the Vocus for most SVOC with 3 to 5 oxygen atoms, while the Nitrate
671 detected mainly products with 6 or more oxygen atoms. No dimer species were observed with either of the
672 PTR instruments, which might be due to wall losses (likely at least for the PTR-TOF) and/or potential
673 fragmentation in the instruments. The Amine CI-APi-TOF is a promising technique, as shown in earlier
674 studies, but it likely requires low loadings in order to not titrate the reagent ion, limiting its utility for many
675 chamber experiments and, potentially, atmospheric observations. The large uncertainties in attempting a
676 quantification of the wide variety of species measurable with these mass spectrometers underline the urgent
677 need of developing robust, simple and complete calibration methods in order to obtain a better estimation of
678 the concentrations. Finally, it is important to underline that the experimental and analytical procedures

679 performed by the user will ultimately impact the sensitivity, the selectivity, and the interpretability of the
680 results attainable from each instrument.

681

682 Data availability

683 All data are available by contacting the corresponding authors.

684

685 Acknowledgments

686 This work was supported by the European Research Council (ERC-StG COALA, grant nr 638703). We
687 gratefully acknowledge Pasi Aalto, Petri Keronen, Frans Korhonen, and Erkki Siivola for technical support.

688 O.G. thanks Doctoral Programme in Atmospheric Sciences (ATM-DP) at the University of Helsinki for
689 financial support. O.P. would like to thank the Vilho, Yrjö and Kalle Väisälä Foundation. We thank the
690 tofTools team for providing tools for mass spectrometry data analysis.

691

692 Author contributions

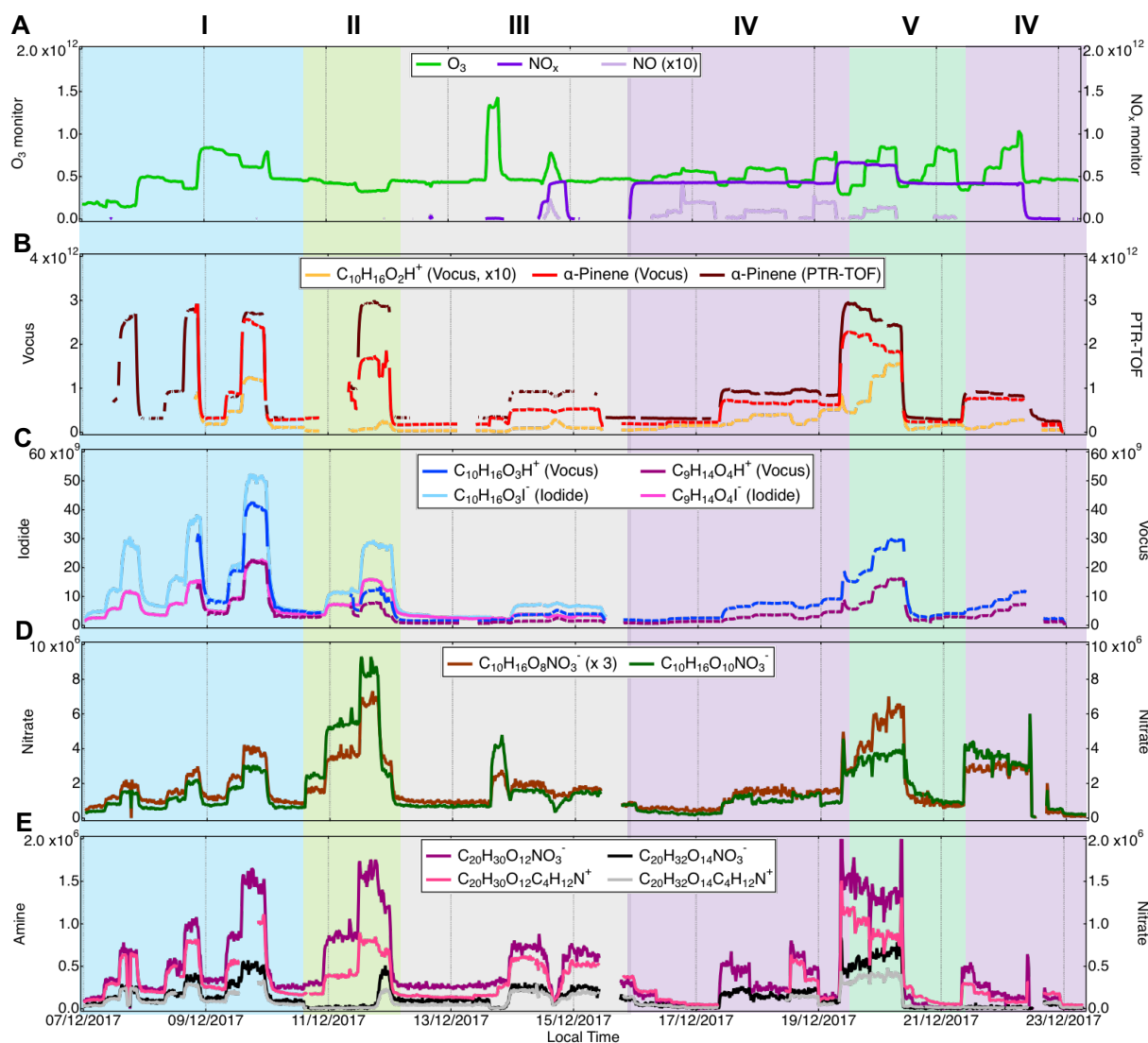
693 M.R. and M.E. designed the experiments. Instrument deployment, operation, and data analysis were carried
694 out by: M.R., P.R. J.E.K., O.P., Y.Z., L.H., O.G. C.Y., and M.E.; M.R., P.R., O.P., and M.E., interpreted the
695 compiled data set. M.R., P. R. and M.E. wrote the paper. All co-authors discussed the results and commented
696 the manuscript. The authors declare that they have no conflict of interest.

697 **Table. 1** Overview and characteristics of the mass spectrometers deployed during the campaign at the COALA
 698 chamber.

Instrument ^a	Ionization ^b	Resolving power ^c	Sampling flow rate (L/min)	T in IMR ^d (°C)	Residence time in IMR	IMR pressure (mbar)	Inlet length (m)
PTR-TOF	Proton transfer	4500	0.8	60	100 μs	2.0	2
Vocus	Proton transfer	12000	4.5	30	82 μs	1.0	1
Iodide	I ⁻ adduct	4500	2	40	94 ms	100	1
Amine	C ₄ H ₁₂ N ⁺ adduct	10000	10	Ambient	200 ms	Ambient	1
Nitrate	NO ₃ ⁻ adduct	9000	10	Ambient	200 ms	Ambient	1

699 ^a The reagent ion is used as a synonym to name the instrument ^b Type of ionization method used for each
 700 instrument; ^c corresponds to the mass resolution of the instruments under the conditions used in this study. ^d
 701 IMR = Ion-molecule reaction chamber, i.e. the region where sample molecules are mixed with reagent ions.
 702 The IMR has a different design in each of the instruments, except for the Nitrate and Amine, which are
 703 identical.

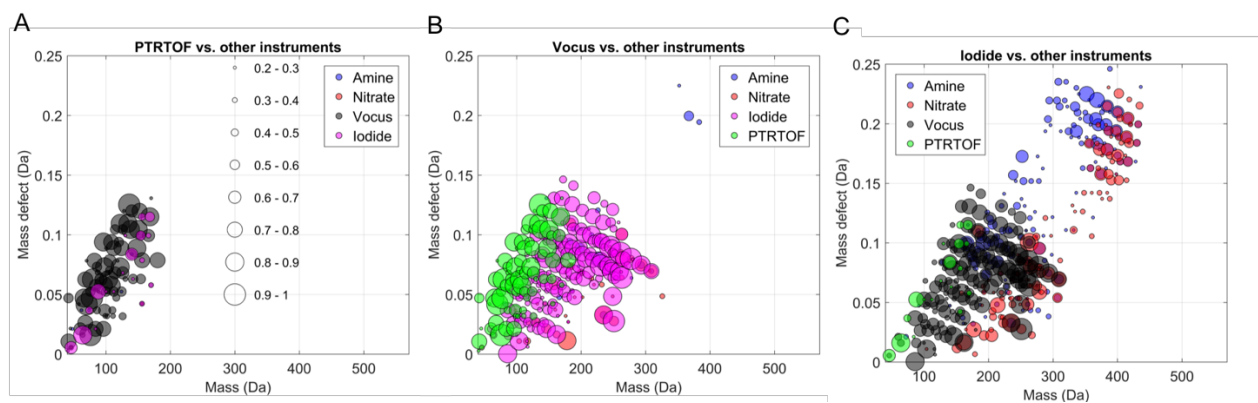
704



706

707 **Figure 1:** Campaign overview, including the concentration of O_3 , NO , NO_x (A) as well as α -pinene measured
 708 by the Vocus and the PTR-TOF and pinonaldehyde measured using the Vocus (B). Concentrations of pinonic
 709 and pinic acids (Vocus & Iodide) are presented in C, example of HOM monomers from Nitrate (D) and
 710 example of HOM dimers from Amine and Nitrate (E). Concentrations for all the gaseous species are in
 711 molecules cm^{-3} , see text for details on quantification. The experiments were separated in 5 types: I: α -pinene
 712 + O_3 ; II: α -pinene + O_3 + CO (as an OH scavenger); III: tests (NO_2 injection, H_2O_2 injection to generate HO_2);
 713 IV: α -pinene + O_3 + NO and V: α -pinene + O_3 + NO + CO. Concentrations of NO and $C_{10}H_{16}O_8NO_3^-$ are scaled
 714 for clarity.

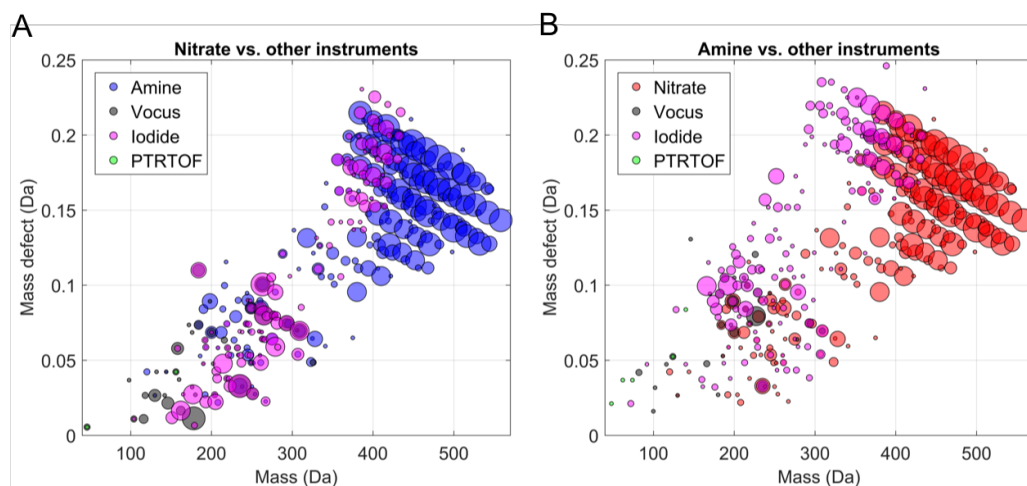
715



716

717 **Figure 2:** Mass defect plots showing the compounds for which time series correlation ($R^2 > 0.2$) was observed
 718 by the medium-pressure chemical ionization mass spectrometers (A) PTR-TOF, (B) Vocus and (C) Iodide.
 719 Each circle represents a distinct molecular composition and the marker area represents the correlation (R^2 ,
 720 legend shown in A) of the time series of that molecule between two different CIMS instruments. The color of
 721 each marker depicts the instrument against which the correlation is calculated.

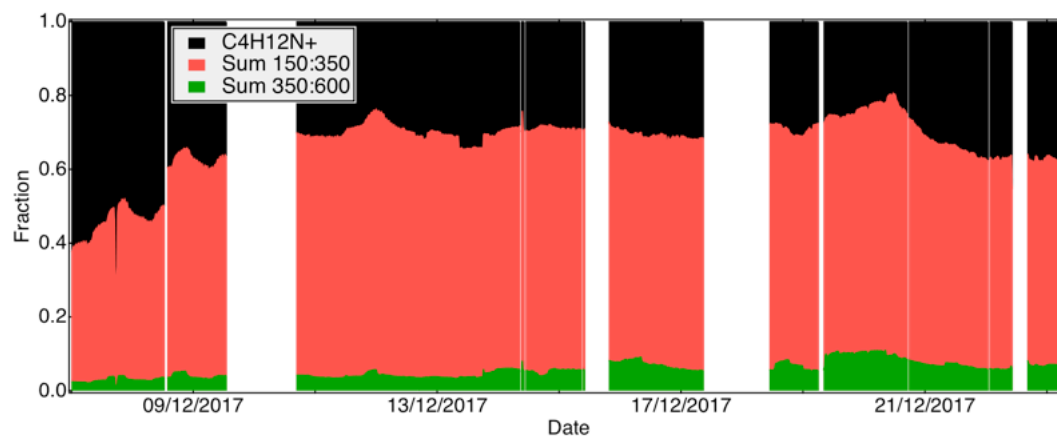
722



723

724 **Figure 3:** Mass defect plots showing the compounds for which time series correlation ($R^2 > 0.2$) was observed
 725 by the atmospheric-pressure chemical ionization mass spectrometers (A) Nitrate and (B) Amine. Each circle
 726 represents a distinct molecular composition and the marker area represents the correlation (R^2 , legend shown
 727 in Figure 2A) of the time series of that molecule between two different CIMS instruments. The color of each
 728 marker depicts the instrument against which the correlation is calculated.

729



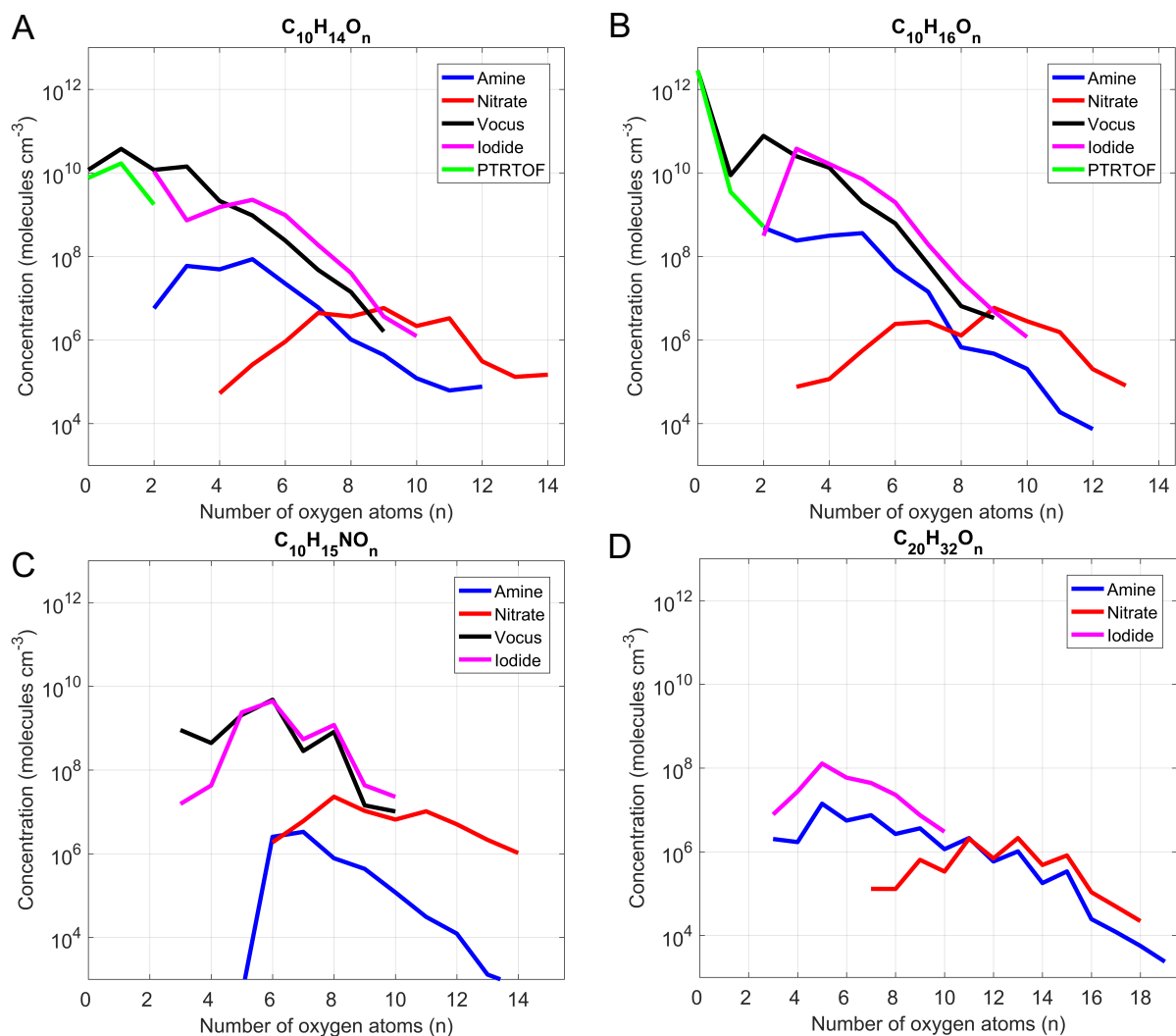
730

731 **Figure 4:** Contribution of the reagent ion, sum of ions from 150 to 350 Th and sum of ions from 350 to 600

732 Th to total ion count throughout the campaign for the Amine CI-APi-TOF. Only a negligible fraction of the

733 signal was found below 150 Th (excluding $C_4H_{12}N^+$).

734



735

736

737

738

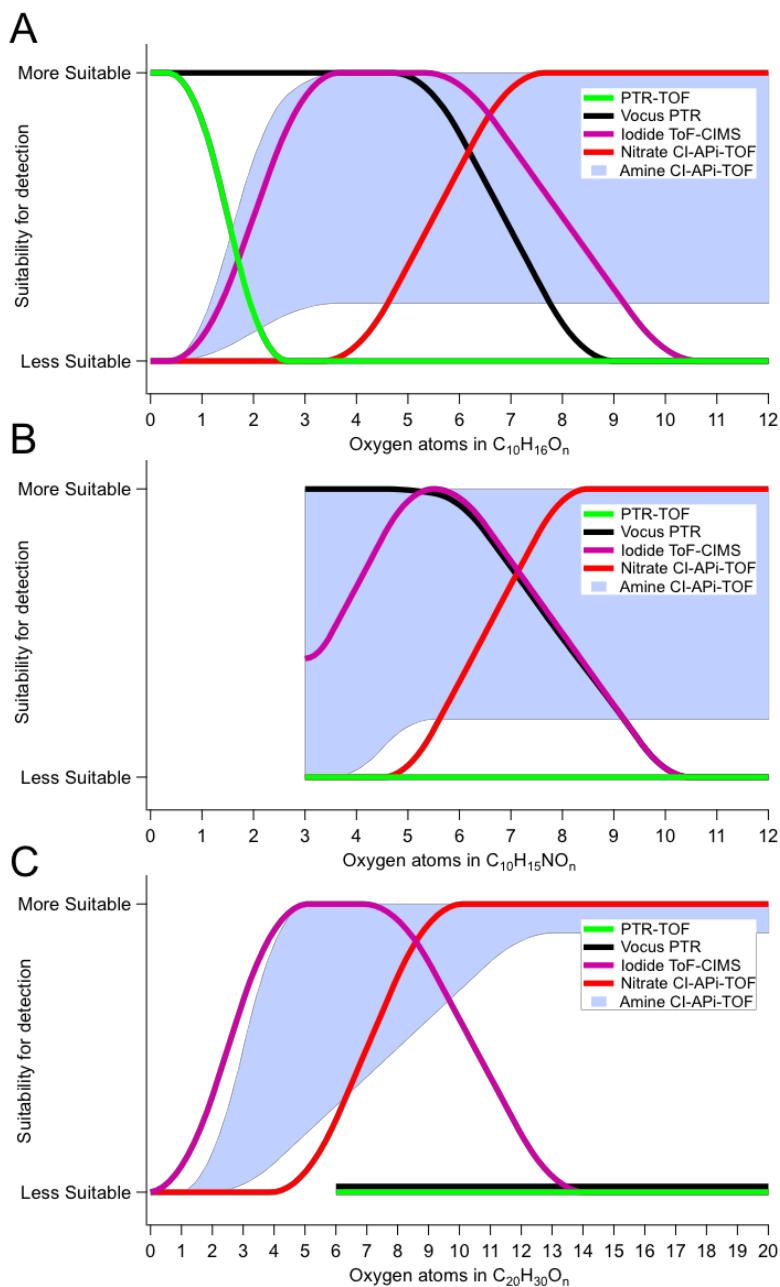
739

740

741

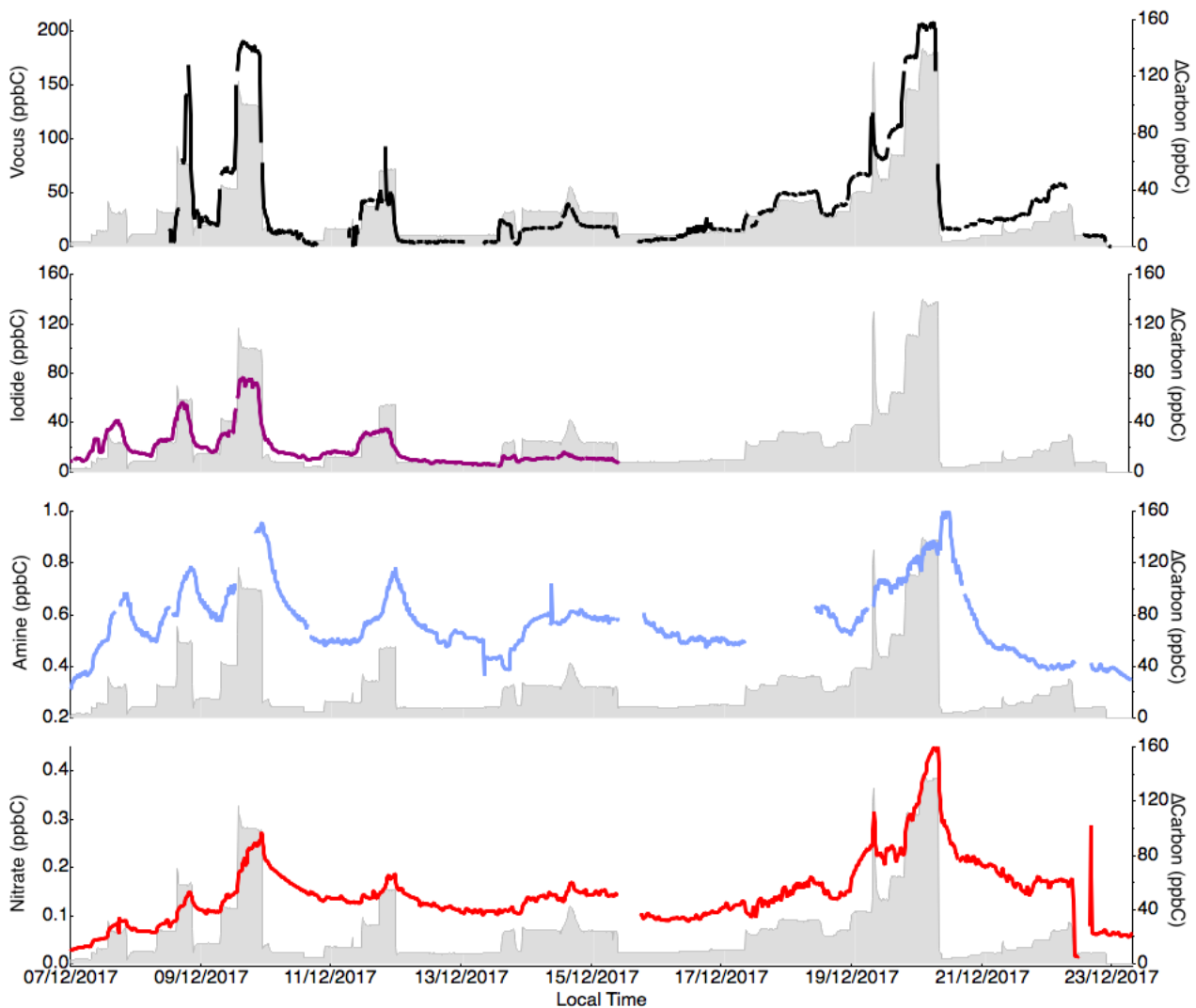
742

Figure 5: Estimated concentrations of the main α -pinene C_{10} -monomer oxidation products (A & B), C_{10} -monomer organonitrates (C) and α -pinene dimers (D) by the different mass spectrometers deployed in this study. The average concentrations were estimated when the system reached steady state in two experiments: without NO (panels A, B & D), December 9 (15:30-23:00) and with NO (panel C), December 20 (02:45 to 07:45). See text for more details. Data is plotted only for ions for which the average concentrations were higher than 3 times the standard deviation during the campaign.



743

744 **Figure 6:** Estimated detection suitability of the different CIMS techniques for α -pinene and its oxidation
 745 products, plotted as a function of the number of oxygen atoms. Each panel symbolizes a compound group:
 746 monomers (A), organonitrate monomers (B) and dimers (C). The figures are indicative only, as none of the
 747 reagent ion chemistries are direct functions of the oxygen atom content in the molecules. See text for more
 748 details.



749

750 **Figure 7:** Concentration (in ppbC) of the sum of the compounds measured by each instrument (Vocus, Iodide,
 751 Amine and Nitrate) throughout the campaign, compared to the amount of reacted carbon through α -pinene
 752 oxidation. Large uncertainties remain in the quantification of the OVOC for all instruments, but it is clear that
 753 the Iodide and Vocus are able to measure a large fraction of the reacted carbon in the gas phase.

754

755 **REFERENCES**

- 756 Albrecht, B. A.: Aerosols, Cloud Microphysics, and Fractional Cloudiness, *Science*, 245(4923), 1227–1230,
757 doi:10.1126/science.245.4923.1227, 1989.
- 758 Atkinson, R., Baulch, D. L., Cox, R. A., Hampson, R. F., Kerr, J. A., Rossi, M. J. and Troe, J.: Evaluated
759 Kinetic and Photochemical Data for Atmospheric Chemistry: Supplement VI. IUPAC Subcommittee on Gas
760 Kinetic Data Evaluation for Atmospheric Chemistry, *Journal of Physical and Chemical Reference Data*, 26(6),
761 1329–1499, doi:10.1063/1.556010, 1997.
- 762 Berndt, T., Richters, S., Kaethner, R., Voigtländer, J., Stratmann, F., Sipilä, M., Kulmala, M. and Herrmann,
763 H.: Gas-Phase Ozonolysis of Cycloalkenes: Formation of Highly Oxidized RO₂ Radicals and Their Reactions
764 with NO, NO₂, SO₂, and Other RO₂ Radicals, *The Journal of Physical Chemistry A*, 119(41), 10336–10348,
765 doi:10.1021/acs.jpca.5b07295, 2015.
- 766 Berndt, T., Herrmann, H. and Kurtén, T.: Direct Probing of Criegee Intermediates from Gas-Phase Ozonolysis
767 Using Chemical Ionization Mass Spectrometry, *Journal of the American Chemical Society*, 139(38), 13387–
768 13392, doi:10.1021/jacs.7b05849, 2017.
- 769 Berndt, T., Scholz, W., Mentler, B., Fischer, L., Herrmann, H., Kulmala, M. and Hansel, A.: Accretion Product
770 Formation from Self- and Cross-Reactions of RO₂ Radicals in the Atmosphere, *Angewandte Chemie*
771 *International Edition*, 57(14), 3820–3824, doi:10.1002/anie.201710989, 2018.
- 772 Bertram, T. H., Kimmel, J. R., Crisp, T. A., Ryder, O. S., Yatavelli, R. L. N., Thornton, J. A., Cubison, M. J.,
773 Gonin, M. and Worsnop, D. R.: A field-deployable, chemical ionization time-of-flight mass spectrometer,
774 *Atmospheric Measurement Techniques*, 4(7), 1471–1479, doi:10.5194/amt-4-1471-2011, 2011.
- 775 Breitenlechner, M., Fischer, L., Hainer, M., Heinritzi, M., Curtius, J. and Hansel, A.: PTR3: An Instrument for
776 Studying the Lifecycle of Reactive Organic Carbon in the Atmosphere, *Analytical Chemistry*, 89(11), 5824–
777 5831, doi:10.1021/acs.analchem.6b05110, 2017.
- 778 Crouse, J. D., McKinney, K. A., Kwan, A. J. and Wennberg, P. O.: Measurement of Gas-Phase
779 Hydroperoxides by Chemical Ionization Mass Spectrometry, *Analytical Chemistry*, 78(19), 6726–6732,
780 doi:10.1021/ac0604235, 2006.
- 781 Cubison, M. J. and Jimenez, J. L.: Statistical precision of the intensities retrieved from constrained fitting of
782 overlapping peaks in high-resolution mass spectra, *Atmospheric Measurement Techniques*, 8(6), 2333–2345,
783 doi:10.5194/amt-8-2333-2015, 2015.
- 784 Docherty, K. S., Wu, W., Lim, Y. B. and Ziemann, P. J.: Contributions of Organic Peroxides to Secondary
785 Aerosol Formed from Reactions of Monoterpenes with O₃, *Environmental Science & Technology*, 39(11),
786 4049–4059, doi:10.1021/es050228s, 2005.
- 787 Donahue, N. M., Robinson, A. L., Trump, E. R., Riipinen, I. and Kroll, J. H.: Volatility and Aging of
788 Atmospheric Organic Aerosol, in *Atmospheric and Aerosol Chemistry*, vol. 339, edited by V. F. McNeill and
789 P. A. Ariya, pp. 97–143, Springer Berlin Heidelberg, Berlin, Heidelberg., 2012.
- 790 Ehn, M., Thornton, J. A., Kleist, E., Sipilä, M., Junninen, H., Pullinen, I., Springer, M., Rubach, F., Tillmann,
791 R., Lee, B., Lopez-Hilfiker, F., Andres, S., Acir, I.-H., Rissanen, M., Jokinen, T., Schobesberger, S.,
792 Kangasluoma, J., Kontkanen, J., Nieminen, T., Kurtén, T., Nielsen, L. B., Jørgensen, S., Kjaergaard, H. G.,
793 Canagaratna, M., Maso, M. D., Berndt, T., Petäjä, T., Wahner, A., Kerminen, V.-M., Kulmala, M., Worsnop,
794 D. R., Wildt, J. and Mentel, T. F.: A large source of low-volatility secondary organic aerosol, *Nature*,
795 506(7489), 476–479, doi:10.1038/nature13032, 2014.
- 796 Gakidou, E., Afshin, A., Abajobir, A. A., Abate, K. H., Abbafati, C., Abbas, K. M., Abd-Allah, F., Abdulle,
797 A. M., Abera, S. F., Aboyans, V., Abu-Raddad, L. J., Abu-Rmeileh, N. M. E., Abyu, G. Y., Adedeji, I. A.,

798 Adetokunboh, O., Afarideh, M., Agrawal, A., Agrawal, S., Ahmadieh, H., Ahmed, M. B., Aichour, M. T. E.,
799 Aichour, A. N., Aichour, I., Akinyemi, R. O., Akseer, N., Alahdab, F., Al-Aly, Z., Alam, K., Alam, N., Alam,
800 T., Alasfoor, D., Alene, K. A., Ali, K., Alizadeh-Navaei, R., Alkerwi, A., Alla, F., Allebeck, P., Al-Raddadi,
801 R., Alsharif, U., Altirkawi, K. A., Alvis-Guzman, N., Amare, A. T., Amini, E., Ammar, W., Amoako, Y. A.,
802 Ansari, H., Antó, J. M., Antonio, C. A. T., Anwari, P., Arian, N., Årnlöv, J., Artaman, A., Aryal, K. K.,
803 Asayesh, H., Asgedom, S. W., Atey, T. M., Avila-Burgos, L., Avokpaho, E. F. G. A., Awasthi, A., Azzopardi,
804 P., Bacha, U., Badawi, A., Balakrishnan, K., Ballew, S. H., Barac, A., Barber, R. M., Barker-Collo, S. L.,
805 Bärnighausen, T., Barquera, S., Barregard, L., Barrero, L. H., Batis, C., Battle, K. E., Baumgarner, B. R.,
806 Baune, B. T., Beardsley, J., Bedi, N., Beghi, E., Bell, M. L., Bennett, D. A., Bennett, J. R., Bensenor, I. M.,
807 Berhane, A., Berhe, D. F., Bernabé, E., Betsu, B. D., Beuran, M., Beyene, A. S., Bhansali, A., Bhutta, Z. A.,
808 Bicer, B. K., Bikbov, B., Birungi, C., Biryukov, S., Blosser, C. D., Boneya, D. J., Bou-Orm, I. R., Brauer, M.,
809 Breitborde, N. J. K., et al.: Global, regional, and national comparative risk assessment of 84 behavioural,
810 environmental and occupational, and metabolic risks or clusters of risks, 1990–2016: a systematic analysis for
811 the Global Burden of Disease Study 2016, *The Lancet*, 390(10100), 1345–1422, doi:10.1016/S0140-
812 6736(17)32366-8, 2017.

813 Glasius, M. and Goldstein, A. H.: Recent Discoveries and Future Challenges in Atmospheric Organic
814 Chemistry, *Environmental Science & Technology*, 50(6), 2754–2764, doi:10.1021/acs.est.5b05105, 2016.

815 Goldstein, A. H. and Galbally, I. E.: Known and Unexplored Organic Constituents in the Earth’s Atmosphere,
816 *Environmental Science & Technology*, 41(5), 1514–1521, doi:10.1021/es072476p, 2007.

817 Graus, M., Müller, M. and Hansel, A.: High Resolution PTR-TOF: Quantification and Formula Confirmation
818 of VOC in Real Time, *Journal of the American Society for Mass Spectrometry*, 21(6), 1037–1044,
819 doi:10.1016/j.jasms.2010.02.006, 2010.

820 Hallquist, M., Wenger, J. C., Baltensperger, U., Rudich, Y., Simpson, D., Claeys, M., Dommen, J., Donahue,
821 N. M., George, C., Goldstein, A. H., Hamilton, J. F., Herrmann, H., Hoffmann, T., Iinuma, Y., Jang, M.,
822 Jenkin, M. E., Jimenez, J. L., Kiendler-Scharr, A., Maenhaut, W., McFiggans, G., Mentel, T. F., Monod, A.,
823 Prévôt, A. S. H., Seinfeld, J. H., Surratt, J. D., Szmigielski, R. and Wildt, J.: The formation, properties and
824 impact of secondary organic aerosol: current and emerging issues, *Atmospheric Chemistry and Physics*, 9(14),
825 5155–5236, doi:10.5194/acp-9-5155-2009, 2009.

826 Hansel, A., Scholz, W., Mentler, B., Fischer, L. and Berndt, T.: Detection of RO₂ radicals and other products
827 from cyclohexene ozonolysis with NH₄⁺ and acetate chemical ionization mass spectrometry, *Atmospheric*
828 *Environment*, 186, 248–255, doi:10.1016/j.atmosenv.2018.04.023, 2018.

829 Heinritzi, M., Simon, M., Steiner, G., Wagner, A. C., Kürten, A., Hansel, A. and Curtius, J.: Characterization
830 of the mass-dependent transmission efficiency of a CIMS, *Atmospheric Measurement Techniques*, 9(4), 1449–
831 1460, doi:10.5194/amt-9-1449-2016, 2016.

832 Hyttinen, N., Kupiainen-Määttä, O., Rissanen, M. P., Muuronen, M., Ehn, M. and Kurtén, T.: Modeling the
833 Charging of Highly Oxidized Cyclohexene Ozonolysis Products Using Nitrate-Based Chemical Ionization,
834 *The Journal of Physical Chemistry A*, 119(24), 6339–6345, doi:10.1021/acs.jpca.5b01818, 2015.

835 Hyttinen, N., Otkjær, R. V., Iyer, S., Kjaergaard, H. G., Rissanen, M. P., Wennberg, P. O. and Kurtén, T.:
836 Computational Comparison of Different Reagent Ions in the Chemical Ionization of Oxidized Multifunctional
837 Compounds, *The Journal of Physical Chemistry A*, 122(1), 269–279, doi:10.1021/acs.jpca.7b10015, 2018.

838 Intergovernmental Panel on Climate Change, Ed.: *Climate Change 2013 - The Physical Science Basis:*
839 *Working Group I Contribution to the Fifth Assessment Report of the Intergovernmental Panel on Climate*
840 *Change*, Cambridge University Press, Cambridge, 2014.

841 Isaacman-VanWertz, G., Massoli, P., O’Brien, R. E., Nowak, J. B., Canagaratna, M. R., Jayne, J. T., Worsnop,
842 D. R., Su, L., Knopf, D. A., Misztal, P. K., Arata, C., Goldstein, A. H. and Kroll, J. H.: Using advanced mass

843 spectrometry techniques to fully characterize atmospheric organic carbon: current capabilities and remaining
844 gaps, *Faraday Discussions*, 200, 579–598, doi:10.1039/C7FD00021A, 2017.

845 Isaacman-VanWertz, G., Massoli, P., O'Brien, R., Lim, C., Franklin, J. P., Moss, J. A., Hunter, J. F., Nowak,
846 J. B., Canagaratna, M. R., Misztal, P. K., Arata, C., Roscioli, J. R., Herndon, S. T., Onasch, T. B., Lambe, A.
847 T., Jayne, J. T., Su, L., Knopf, D. A., Goldstein, A. H., Worsnop, D. R. and Kroll, J. H.: Chemical evolution
848 of atmospheric organic carbon over multiple generations of oxidation, *Nature Chemistry*, 10(4), 462–468,
849 doi:10.1038/s41557-018-0002-2, 2018.

850 Iyer, S., Lopez-Hilfiker, F., Lee, B. H., Thornton, J. A. and Kurtén, T.: Modeling the Detection of Organic and
851 Inorganic Compounds Using Iodide-Based Chemical Ionization, *The Journal of Physical Chemistry A*, 120(4),
852 576–587, doi:10.1021/acs.jpca.5b09837, 2016.

853 Iyer, S., He, X., Hyttinen, N., Kurtén, T. and Rissanen, M. P.: Computational and Experimental Investigation
854 of the Detection of HO₂ Radical and the Products of Its Reaction with Cyclohexene Ozonolysis Derived RO
855 ₂ Radicals by an Iodide-Based Chemical Ionization Mass Spectrometer, *The Journal of Physical Chemistry A*,
856 121(36), 6778–6789, doi:10.1021/acs.jpca.7b01588, 2017.

857 Jimenez, J. L., Canagaratna, M. R., Donahue, N. M., Prevot, A. S. H., Zhang, Q., Kroll, J. H., DeCarlo, P. F.,
858 Allan, J. D., Coe, H., Ng, N. L., Aiken, A. C., Docherty, K. S., Ulbrich, I. M., Grieshop, A. P., Robinson, A.
859 L., Duplissy, J., Smith, J. D., Wilson, K. R., Lanz, V. A., Hueglin, C., Sun, Y. L., Tian, J., Laaksonen, A.,
860 Raatikainen, T., Rautiainen, J., Vaattovaara, P., Ehn, M., Kulmala, M., Tomlinson, J. M., Collins, D. R.,
861 Cubison, M. J., E., Dunlea, J., Huffman, J. A., Onasch, T. B., Alfarra, M. R., Williams, P. I., Bower, K., Kondo,
862 Y., Schneider, J., Drewnick, F., Borrmann, S., Weimer, S., Demerjian, K., Salcedo, D., Cottrell, L., Griffin,
863 R., Takami, A., Miyoshi, T., Hatakeyama, S., Shimono, A., Sun, J. Y., Zhang, Y. M., Dzepina, K., Kimmel, J.
864 R., Sueper, D., Jayne, J. T., Herndon, S. C., Trimborn, A. M., Williams, L. R., Wood, E. C., Middlebrook, A.
865 M., Kolb, C. E., Baltensperger, U. and Worsnop, D. R.: Evolution of Organic Aerosols in the Atmosphere,
866 *Science*, 326(5959), 1525–1529, doi:10.1126/science.1180353, 2009.

867 Jokinen, T., Sipilä, M., Junninen, H., Ehn, M., Lönn, G., Hakala, J., Petäjä, T., Mauldin, R. L., Kulmala, M.
868 and Worsnop, D. R.: Atmospheric sulphuric acid and neutral cluster measurements using CI-APi-TOF,
869 *Atmospheric Chemistry and Physics*, 12(9), 4117–4125, doi:10.5194/acp-12-4117-2012, 2012.

870 Jokinen, T., Sipilä, M., Richters, S., Kerminen, V.-M., Paasonen, P., Stratmann, F., Worsnop, D., Kulmala,
871 M., Ehn, M., Herrmann, H. and Berndt, T.: Rapid Autoxidation Forms Highly Oxidized RO₂ Radicals in the
872 Atmosphere, *Angewandte Chemie International Edition*, 53(52), 14596–14600, doi:10.1002/anie.201408566,
873 2014.

874 Jokinen, T., Berndt, T., Makkonen, R., Kerminen, V.-M., Junninen, H., Paasonen, P., Stratmann, F., Herrmann,
875 H., Guenther, A. B., Worsnop, D. R., Kulmala, M., Ehn, M. and Sipilä, M.: Production of extremely low
876 volatile organic compounds from biogenic emissions: Measured yields and atmospheric implications,
877 *Proceedings of the National Academy of Sciences*, 112(23), 7123–7128, doi:10.1073/pnas.1423977112, 2015.

878 Jordan, A., Haidacher, S., Hanel, G., Hartungen, E., Märk, L., Seehauser, H., Schottkowsky, R., Sulzer, P. and
879 Märk, T. D.: A high resolution and high sensitivity proton-transfer-reaction time-of-flight mass spectrometer
880 (PTR-TOF-MS), *International Journal of Mass Spectrometry*, 286(2), 122–128,
881 doi:10.1016/j.ijms.2009.07.005, 2009.

882 Junninen, H., Ehn, M., Petäjä, T., Luosujärvi, L., Kotiaho, T., Kostianinen, R., Rohner, U., Gonin, M., Fuhrer,
883 K., Kulmala, M. and Worsnop, D. R.: A high-resolution mass spectrometer to measure atmospheric ion
884 composition, *Atmospheric Measurement Techniques*, 3(4), 1039–1053, doi:10.5194/amt-3-1039-2010, 2010.

885 Kelly, J. M., Doherty, R. M., O'Connor, F. M. and Mann, G. W.: The impact of biogenic,
886 anthropogenic, and biomass burning volatile organic compound emissions on regional and seasonal variations
887 in secondary organic aerosol, *Atmospheric Chemistry and Physics*, 18(10), 7393–7422, doi:10.5194/acp-18-

888 7393-2018, 2018.

889 Kirkby, J., Duplissy, J., Sengupta, K., Frege, C., Gordon, H., Williamson, C., Heinritzi, M., Simon, M., Yan,
890 C., Almeida, J., Tröstl, J., Nieminen, T., Ortega, I. K., Wagner, R., Adamov, A., Amorim, A., Bernhammer,
891 A.-K., Bianchi, F., Breitenlechner, M., Brilke, S., Chen, X., Craven, J., Dias, A., Ehrhart, S., Flagan, R. C.,
892 Franchin, A., Fuchs, C., Guida, R., Hakala, J., Hoyle, C. R., Jokinen, T., Junninen, H., Kangasluoma, J., Kim,
893 J., Krapf, M., Kürten, A., Laaksonen, A., Lehtipalo, K., Makhmutov, V., Mathot, S., Molteni, U., Onnela, A.,
894 Peräkylä, O., Piel, F., Petäjä, T., Praplan, A. P., Pringle, K., Rap, A., Richards, N. A. D., Riipinen, I., Rissanen,
895 M. P., Rondo, L., Sarnela, N., Schobesberger, S., Scott, C. E., Seinfeld, J. H., Sipilä, M., Steiner, G., Stozhkov,
896 Y., Stratmann, F., Tomé, A., Virtanen, A., Vogel, A. L., Wagner, A. C., Wagner, P. E., Weingartner, E.,
897 Wimmer, D., Winkler, P. M., Ye, P., Zhang, X., Hansel, A., Dommen, J., Donahue, N. M., Worsnop, D. R.,
898 Baltensperger, U., Kulmala, M., Carslaw, K. S. and Curtius, J.: Ion-induced nucleation of pure biogenic
899 particles, *Nature*, 533(7604), 521–526, doi:10.1038/nature17953, 2016.

900 Krechmer, J., Lopez-Hilfiker, F., Koss, A., Hutterli, M., Stoermer, C., Deming, B., Kimmel, J., Warneke, C.,
901 Holzinger, R., Jayne, J. T., Worsnop, D. R., Fuhrer, K., Gonin, M. and de Gouw, J. A.: Evaluation of a New
902 Reagent-Ion Source and Focusing Ion-Molecule Reactor for use in Proton-Transfer-Reaction Mass
903 Spectrometry, *Analytical Chemistry*, doi:10.1021/acs.analchem.8b02641, 2018.

904 Kürten, A., Rondo, L., Ehrhart, S. and Curtius, J.: Calibration of a Chemical Ionization Mass Spectrometer for
905 the Measurement of Gaseous Sulfuric Acid, *The Journal of Physical Chemistry A*, 116(24), 6375–6386,
906 doi:10.1021/jp212123n, 2012.

907 Lee, A., Goldstein, A. H., Keywood, M. D., Gao, S., Varutbangkul, V., Bahreini, R., Ng, N. L., Flagan, R. C.
908 and Seinfeld, J. H.: Gas-phase products and secondary aerosol yields from the ozonolysis of ten different
909 terpenes, *Journal of Geophysical Research*, 111(D7), doi:10.1029/2005JD006437, 2006.

910 Lee, B. H., Lopez-Hilfiker, F. D., Mohr, C., Kurtén, T., Worsnop, D. R. and Thornton, J. A.: An Iodide-Adduct
911 High-Resolution Time-of-Flight Chemical-Ionization Mass Spectrometer: Application to Atmospheric
912 Inorganic and Organic Compounds, *Environmental Science & Technology*, 48(11), 6309–6317,
913 doi:10.1021/es500362a, 2014.

914 Lee, B. H., Mohr, C., Lopez-Hilfiker, F. D., Lutz, A., Hallquist, M., Lee, L., Romer, P., Cohen, R. C., Iyer, S.,
915 Kurtén, T., Hu, W., Day, D. A., Campuzano-Jost, P., Jimenez, J. L., Xu, L., Ng, N. L., Guo, H., Weber, R. J.,
916 Wild, R. J., Brown, S. S., Koss, A., de Gouw, J., Olson, K., Goldstein, A. H., Seco, R., Kim, S., McAvey, K.,
917 Shepson, P. B., Starn, T., Baumann, K., Edgerton, E. S., Liu, J., Shilling, J. E., Miller, D. O., Brune, W.,
918 Schobesberger, S., D’Ambro, E. L. and Thornton, J. A.: Highly functionalized organic nitrates in the southeast
919 United States: Contribution to secondary organic aerosol and reactive nitrogen budgets, *Proceedings of the*
920 *National Academy of Sciences*, 113(6), 1516–1521, doi:10.1073/pnas.1508108113, 2016.

921 Li, X., Chee, S., Hao, J., Abbatt, J. P. D., Jiang, J. and Smith, J. N.: Relative Humidity Effect on the Formation
922 of Highly Oxidized Molecules and New Particles during Monoterpene Oxidation, *Atmospheric Chemistry and*
923 *Physics Discussions*, 1–26, doi:10.5194/acp-2018-898, 2018.

924 Lindinger, W., Hansel, A. and Jordan, A.: On-line monitoring of volatile organic compounds at pptv levels by
925 means of proton-transfer-reaction mass spectrometry (PTR-MS) medical applications, food control and
926 environmental research, *International Journal of Mass Spectrometry and Ion Processes*, 173(3), 191–241,
927 doi:10.1016/S0168-1176(97)00281-4, 1998.

928 Lopez-Hilfiker, F. D., Iyer, S., Mohr, C., Lee, B. H., D’Ambro, E. L., Kurtén, T. and Thornton, J. A.:
929 Constraining the sensitivity of iodide adduct chemical ionization mass spectrometry to multifunctional organic
930 molecules using the collision limit and thermodynamic stability of iodide ion adducts, *Atmospheric*
931 *Measurement Techniques*, 9(4), 1505–1512, doi:10.5194/amt-9-1505-2016, 2016.

932 Mohr, C., Lopez-Hilfiker, F. D., Yli-Juuti, T., Heitto, A., Lutz, A., Hallquist, M., D’Ambro, E. L., Rissanen,

- 933 M. P., Hao, L., Schobesberger, S., Kulmala, M., Mauldin, R. L., Makkonen, U., Sipilä, M., Petäjä, T. and
934 Thornton, J. A.: Ambient observations of dimers from terpene oxidation in the gas phase: Implications for new
935 particle formation and growth: Ambient Observations of Gas-Phase Dimers, *Geophysical Research Letters*,
936 44(6), 2958–2966, doi:10.1002/2017GL072718, 2017.
- 937 Pagonis, D., Krechmer, J. E., de Gouw, J., Jimenez, J. L. and Ziemann, P. J.: Effects of gas–wall partitioning
938 in Teflon tubing and instrumentation on time-resolved measurements of gas-phase organic compounds,
939 *Atmospheric Measurement Techniques*, 10(12), 4687–4696, doi:10.5194/amt-10-4687-2017, 2017.
- 940 Riva, M., Budisulistiorini, S. H., Zhang, Z., Gold, A., Thornton, J. A., Turpin, B. J. and Surratt, J. D.:
941 Multiphase reactivity of gaseous hydroperoxide oligomers produced from isoprene ozonolysis in the presence
942 of acidified aerosols, *Atmospheric Environment*, 152, 314–322, doi:10.1016/j.atmosenv.2016.12.040, 2017.
- 943 Schallhart, S., Rantala, P., Nemitz, E., Taipale, D., Tillmann, R., Mentel, T. F., Loubet, B., Gerosa, G., Finco,
944 A., Rinne, J. and Ruuskanen, T. M.: Characterization of total ecosystem-scale biogenic VOC exchange at a
945 Mediterranean oak–hornbeam forest, *Atmospheric Chemistry and Physics*, 16(11), 7171–7194,
946 doi:10.5194/acp-16-7171-2016, 2016.
- 947 Schobesberger, S., Junninen, H., Bianchi, F., Lonn, G., Ehn, M., Lehtipalo, K., Dommen, J., Ehrhart, S.,
948 Ortega, I. K., Franchin, A., Nieminen, T., Riccobono, F., Hutterli, M., Duplissy, J., Almeida, J., Amorim, A.,
949 Breitenlechner, M., Downard, A. J., Dunne, E. M., Flagan, R. C., Kajos, M., Keskinen, H., Kirkby, J., Kupc,
950 A., Kurten, A., Kurten, T., Laaksonen, A., Mathot, S., Onnela, A., Praplan, A. P., Rondo, L., Santos, F. D.,
951 Schallhart, S., Schnitzhofer, R., Sipilä, M., Tome, A., Tsagkogeorgas, G., Vehkamäki, H., Wimmer, D.,
952 Baltensperger, U., Carslaw, K. S., Curtius, J., Hansel, A., Petaja, T., Kulmala, M., Donahue, N. M. and
953 Worsnop, D. R.: Molecular understanding of atmospheric particle formation from sulfuric acid and large
954 oxidized organic molecules, *Proceedings of the National Academy of Sciences*, 110(43), 17223–17228,
955 doi:10.1073/pnas.1306973110, 2013.
- 956 Stark, H., Yatavelli, R. L. N., Thompson, S. L., Kimmel, J. R., Cubison, M. J., Chhabra, P. S., Canagaratna,
957 M. R., Jayne, J. T., Worsnop, D. R. and Jimenez, J. L.: Methods to extract molecular and bulk chemical
958 information from series of complex mass spectra with limited mass resolution, *International Journal of Mass
959 Spectrometry*, 389, 26–38, doi:10.1016/j.ijms.2015.08.011, 2015.
- 960 Stark, H., Yatavelli, R. L. N., Thompson, S. L., Kang, H., Krechmer, J. E., Kimmel, J. R., Palm, B. B., Hu,
961 W., Hayes, P. L., Day, D. A., Campuzano-Jost, P., Canagaratna, M. R., Jayne, J. T., Worsnop, D. R. and
962 Jimenez, J. L.: Impact of Thermal Decomposition on Thermal Desorption Instruments: Advantage of
963 Thermogram Analysis for Quantifying Volatility Distributions of Organic Species, *Environmental Science &
964 Technology*, 51(15), 8491–8500, doi:10.1021/acs.est.7b00160, 2017.
- 965 Tröstl, J., Chuang, W. K., Gordon, H., Heinritzi, M., Yan, C., Molteni, U., Ahlm, L., Frege, C., Bianchi, F.,
966 Wagner, R., Simon, M., Lehtipalo, K., Williamson, C., Craven, J. S., Duplissy, J., Adamov, A., Almeida, J.,
967 Bernhammer, A.-K., Breitenlechner, M., Brilke, S., Dias, A., Ehrhart, S., Flagan, R. C., Franchin, A., Fuchs,
968 C., Guida, R., Gysel, M., Hansel, A., Hoyle, C. R., Jokinen, T., Junninen, H., Kangasluoma, J., Keskinen, H.,
969 Kim, J., Krapf, M., Kürten, A., Laaksonen, A., Lawler, M., Leiminger, M., Mathot, S., Möhler, O., Nieminen,
970 T., Onnela, A., Petäjä, T., Piel, F. M., Miettinen, P., Rissanen, M. P., Rondo, L., Sarnela, N., Schobesberger,
971 S., Sengupta, K., Sipilä, M., Smith, J. N., Steiner, G., Tomè, A., Virtanen, A., Wagner, A. C., Weingartner, E.,
972 Wimmer, D., Winkler, P. M., Ye, P., Carslaw, K. S., Curtius, J., Dommen, J., Kirkby, J., Kulmala, M.,
973 Riipinen, I., Worsnop, D. R., Donahue, N. M. and Baltensperger, U.: The role of low-volatility organic
974 compounds in initial particle growth in the atmosphere, *Nature*, 533(7604), 527–531,
975 doi:10.1038/nature18271, 2016.
- 976 Twomey, S.: The Influence of Pollution on the Shortwave Albedo of Clouds, *Journal of the Atmospheric
977 Sciences*, 34(7), 1149–1152, doi:10.1175/1520-0469(1977)034<1149:TIOPOT>2.0.CO;2, 1977.
- 978 Wang, S., Riva, M., Yan, C., Ehn, M. and Wang, L.: Primary Formation of Highly Oxidized Multifunctional

- 979 Products in the OH-Initiated Oxidation of Isoprene. A Combined Theoretical and Experimental Study,
980 Environmental Science & Technology, doi:10.1021/acs.est.8b02783, 2018.
- 981 Yuan, B., Koss, A. R., Warneke, C., Coggon, M., Sekimoto, K. and de Gouw, J. A.: Proton-Transfer-Reaction
982 Mass Spectrometry: Applications in Atmospheric Sciences, Chemical Reviews, 117(21), 13187–13229,
983 doi:10.1021/acs.chemrev.7b00325, 2017.
- 984 Ziemann, P. J. and Atkinson, R.: Kinetics, products, and mechanisms of secondary organic aerosol formation,
985 Chemical Society Reviews, 41(19), 6582, doi:10.1039/c2cs35122f, 2012.
- 986